ANESTHESIOLOGY

GABAergic Neurons in the Dorsal–Intermediate Lateral Septum Regulate Sleep–Wakefulness and Anesthesia in Mice

Di Wang, M.D., Qingchen Guo, Ph.D., Yu Zhou, M.D., Zheng Xu, M.D., Su-Wan Hu, M.D., Xiang-Xi Kong, M.D., Yu-Mei Yu, M.D., Jun-Xia Yang, M.D., Hongxing Zhang, M.D., Ph.D., Hai-Lei Ding, M.D., Ph.D., Jun-Li Cao, M.D., Ph.D.

ANESTHESIOLOGY 2021; 135:463–81

EDITOR'S PERSPECTIVE

What We Already Know about This Topic

- The lateral septum of the brain is known to play a key role in emotional processes and stress responses
- Inhibitory γ-aminobutyric acid–mediated neurons of the lateral septum send synaptic connections to multiple brain regions involved in the regulation of sleep/wakefulness
- The role of the lateral septum in the regulation of sleep/wakefulness is incompletely understood

What This Article Tells Us That Is New

- A combination of genetic and electrophysiologic techniques in male mice revealed that γ-aminobutyric acid–mediated neurons of the lateral septum are highly active during the awake state
- Genetic activation of γ-aminobutyric acid–mediated neurons in the lateral septum promotes recovery from isoflurane anesthesia through the projection of these cells to the ventral tegmental area
- These observations suggest a role for γ-aminobutyric acid–mediated neurons in the lateral septum to maintain wakefulness and to promote recovery from isoflurane anesthesia

ABSTRACT

Background: The γ-aminobutyric acid–mediated (GABAergic) inhibitory system in the brain is critical for regulation of sleep–wake and general anesthesia. The lateral septum contains mainly GABAergic neurons, being cytoarchitectonically divided into the dorsal, intermediate, and ventral parts. This study hypothesized that GABAergic neurons of the lateral septum participate in the control of wakefulness and promote recovery from anesthesia.

Methods: By employing fiber photometry, chemogenetic and optogenetic neuronal manipulations, anterograde tracing, *in vivo* electrophysiology, and electroencephalogram/electromyography recordings in adult male mice, the authors measured the role of lateral septum GABAergic neurons to the control of sleep–wake transition and anesthesia emergence and the corresponding neuron circuits in arousal and emergence control.

Results: The GABAergic neurons of the lateral septum exhibited high activities during the awake state by *in vivo* fiber photometry recordings (awake *vs.* non–rapid eye movement sleep: 3.3 ± 1.4% *vs.* –1.3 ± 1.2%, $P < 0.001$, n = 7 mice/group; awake *vs.* anesthesia: 2.6 ± 1.2% *vs.* –1.3 ± 0.8%, $P < 0.001$, n = 7 mice/group). Using chemogenetic stimulation of lateral septum GABAergic neurons resulted in a 100.5% increase in wakefulness and a 51.2% reduction in non–rapid eye movement sleep. Optogenetic activation of these GABAergic neurons promoted wakefulness from sleep (median [25th, 75th percentiles]: 153.0 [115.9, 179.7] s to 4.0 [3.4, 4.6] s, $P = 0.009$, n = 5 mice/group) and accelerated emergence from isoflurane anesthesia (514.4 ± 122.2 s *vs.* 226.5 ± 53.3 s, $P < 0.001$, n = 8 mice/group). Furthermore, the authors demonstrated that the lateral septum GABAergic neurons send 70.7% (228 of 323 cells) of monosynaptic projections to the ventral tegmental area GABAergic neurons, preferentially inhibiting their activities and thus regulating wakefulness and isoflurane anesthesia depth.

Conclusions: The results uncover a fundamental role of the lateral septum GABAergic neurons and their circuit in maintaining awake state and promoting general anesthesia emergence time.

(ANESTHESIOLOGY 2021; 135:463–81)

Sleep–wakefulness cycles are vital physiologic processes. Of note, that one stays in wakefulness is required for motivation-related behaviors. It has been suggested that the lateral septum plays critical roles in regulating motivation-related behaviors, including those involved in exploration[1] and defensive behaviors.[2]

Wakefulness is enabled by aminergic and peptidergic systems involving acetylcholine,[3] dopamine,[4] noradrenaline,[5] serotonin,[6] histamine,[7] glutamate,[8] γ-aminobutyric acid (GABA),[9] neurotensin,[10] and orexin,[11] whereas sleep requires the γ-aminobutyric acid–mediated (GABAergic)/peptidergic and glutamatergic/nitrergic neurons in the anterior hypothalamus, also known as the sleep-promoting neurons, to inhibit wakefulness-promoting brain regions.[12,13] The lateral septum is largely composed of GABAergic neurons. They send synaptic connections to

Supplemental Digital Content is available for this article. Direct URL citations appear in the printed text and are available in both the HTML and PDF versions of this article. Links to the digital files are provided in the HTML text of this article on the Journal's Web site (www.anesthesiology.org). D.W. and Q.G. contributed equally to this article.

Submitted for publication December 29, 2020. Accepted for publication April 27, 2021. Published online first on July 13, 2021. From Jiangsu Province Key Laboratory of Anesthesiology, Jiangsu Province Key Laboratory of Anesthesia and Analgesia Application Technology, NMPA Key Laboratory for Research and Evaluation of Narcotic and Psychotropic Drugs, Xuzhou Medical University, Xuzhou, China (D.W., Q.G., Y.Z., Z.X., S.-W.H., X.-X.K., Y.-M.Y., J.-X.Y., H.Z., H.-L.D., J.-L.C.) and the Department of Anesthesiology, Affiliated Hospital of Xuzhou Medical University, Xuzhou, China (J.-L.C.).

 Anesthesiology 2021; 135:463–81. DOI: 10.1097/ALN.0000000000003868

<zdoi;. DOI: 10.1097/ALN.0000000000003868>

multiple brain regions, for example, the ventral tegmental area and hypothalamus, which have been demonstrated to regulate wakefulness and motivation.[14,15]

Compelling evidence has indicated that the ventral tegmental area is pivotal to sleep–wakefulness cycles.[4,8] Specifically, the ventral tegmental area dopaminergic circuit regulates sleep-related behaviors and maintains the behavioral and electrocortical awake state,[4] whereas the GABAergic neurons promote non–rapid eye movement (non-REM) sleep.[16] Previous lesion-based and pharmacologic studies have suggested that the lateral septum modulates the activities of the ventral tegmental area dopaminergic neurons by inhibiting GABAergic interneurons.[15] These findings led to our hypothesis that the lateral septum GABAergic neurons may be involved in sleep–wakefulness regulation through the lateral septum-ventral tegmental area circuit.

General anesthesia was discovered more than 170 yr ago, yet the precise mechanisms by which the anesthetics work remain elusive.[17] In the past few decades, the relationship between general anesthesia and sleep has received much attention. Several lines of evidence suggest that these two processes may share some similar cellular and circuitry machineries.[18] For example, sleep is promoted by the activation of the ventrolateral preoptic area.[19] Meanwhile, this region is also found to activate in general anesthesia, which in turn inhibits arousal-promoting circuits.[20,21] As such, we hypothesized that the lateral septum may be involved in both natural sleep–wakefulness and general anesthesia regulation.

Materials and Methods

Animals

Male C57BL/6J wild-type mice were purchased from Jinan Pengyue Laboratory Animal Breeding Co. Ltd. (China), and *Vgat-ires-Cre* transgenic mice were purchased from the Jackson Laboratory (*Vgat*-ires-Cre: *Slc32a1*$^{tm2(cre)Lowl}$*/J*: JAX stock 016962). The mice used for all experiments (heterozygous Tg [*Vgat-Cre*] mice maintained on a *Slc32a1*$^{tm2(cre)Lowl}$*/J*×C57BL/6J genetic background) were housed in individual custom-designed polycarbonate cages at constant temperature (22 ± 1°C), humidity (30 to 50%), and circadian cycle (12-h light–dark cycle, starting at 7 AM). Food and water were available *ad libitum*. All procedures were performed in accordance with standard ethical guidelines in accordance with the National Institutes of Health Guide for the Care and Use of Laboratory Animals and were approved by the Animal Care and Use Committee of Xuzhou Medical University. Only adult male mice were used in the behavioral experiments, whereas adult male and female mice with a similar distribution were used for herpes simplex virus anterograde tracing and *in vivo* electrophysiologic experiments. All mice were aged 8 weeks and weighed 22 to 24 g at the start of the experiments.

Randomization methods were used to assign all mice to the control and experimental groups and were tested in sequential order. Blinding methods were used to prevent investigators, assessors, raters, or other research personnel from knowledge of group assignment when assessing results. No mouse used for behavioral experiments was reused for other assays. A total of 168 mice were recruited for fiber photometry recording and analysis, polygraphic recordings and analysis, general anesthesia experiments immunohistochemistry staining, viral tracing, and *in vivo* electrophysiologic and behavioral experiments in the current study. Of the mice used, 37 mice were excluded because of death, or missed targets, including the injection of viruses and placement of optic fibers. After the behavioral experiments, the virus injection sites and fiber implantation sites were confirmed in all animals, and those with incorrect locations were excluded from the final analyses. At the end of the experiments, all mice were euthanized using carbon dioxide asphyxiation under isoflurane anesthesia.

Stereotaxic Surgery and Viral Injection

Vgat-Cre mice were anesthetized using sodium pentobarbital (50 mg/kg, intraperitoneally) and placed in a stereotaxic apparatus (RWD, China). Their eyes were administered ophthalmic ointment to prevent drying, and a heating pad was used to maintain the body temperature at 35 to 37°C. After shaving off the hair and disinfecting the incision site using iodine and medical alcohol, the scalp was incised to expose the skull, and the connective tissue was gently removed from the skull surface using cotton swabs. Small craniotomy holes (~1 mm in diameter) were drilled with the help of a microscope, and adeno-associated virus (AAV) vectors were injected through a stainless steel 33-gauge/15-mm/PST3 internal cannula attached to a 10-μl syringe (Hamilton, USA) at a rate of 0.1 μl min^{-1}. After injection, the pipette was left in place for an additional 10 min and then slowly retracted. For the fiber photometry experiments, recombinant AAV-Ef1α-DIO-GCaMP6s (200 nl; BrainVTA, China) was injected into the dorsal–intermediate lateral septum unilaterally (coordinates, bregma: anterior–posterior: +0.5 mm; mediolateral: +0.4 mm; dorsal–ventral: −3.0 mm). For the chemogenetic or optogenetic activation or inactivation of dorsal–intermediate lateral septum GABAergic neurons, recombinant AAV-Ef1α-DIO-hM3Dq-mCherry, recombinant AAV–Ef1α–DIO–channelrhodopsin-2 (ChR2)–enhanced yellow fluorescent protein (eYFP), recombinant AAV-Ef1α-DIO-NpHR-eYFP, or recombinant AAV-Ef1α-DIO-eYFP (200 nl; BrainVTA) was injected bilaterally into the dorsal–intermediate lateral septum (coordinates, bregma: anterior–posterior: +0.5 mm; mediolateral: ±0.4 mm; dorsal–ventral: −3.0 mm).

For anterograde monosynaptic projection of dorsal–intermediate lateral septum GABAergic neurons, some mice were injected with the recombinant

AAV-EF1α-DIO-TVA-EGFP helper virus (200 nl; BrainVTA) into the dorsal–intermediate lateral septum unilaterally using the procedures described above, whereas others were also injected with AAV-EF1α-DIO-GFP in the ventral tegmental area (coordinates, bregma: anterior–posterior: −3.2 mm; mediolateral: +0.5 mm; dorsal–ventral: −4.3 mm). Three weeks later, herpes simplex virus vectors H129-ΔTK-tdTomato (100 nl; BrainVTA) were injected into the dorsal–intermediate lateral septum at the same brain location. The animals were allowed to recover from anesthesia under a heating lamp before being returned to their home cage. The mice were housed for an additional week under biosafety level 2 conditions to allow for H129 spread and tdTomato expression.

At 2 weeks after AAV injection, the mice were implanted with electroencephalography (EEG) and electromyography (EMG) electrodes for polysomnographic recordings. EEG and EMG signals were recorded from stainless steel screws inserted into the skull and two flexible silver wires inserted in the neck muscle, respectively. For somatic calcium signal recordings, additional optical fibers (diameter: 200 μm, length: 3.0 mm, numerical aperture: 0.48; Newson, China) were positioned unilaterally in the dorsal–intermediate lateral septum (coordinates, bregma: anterior–posterior: +0.5 mm; mediolateral: +0.4 mm; dorsal–ventral: −2.9 mm); when recording calcium signals at the axons, additional optical fibers (diameter: 200 μm, length: 4.5 mm, numerical aperture: 0.48; Newson) were bilaterally implanted in the ventral tegmental area (coordinates, bregma: anterior–posterior: −3.2 mm; mediolateral: +1.05 mm; dorsal–ventral: −4.4 mm, 7-degree angle). For optical stimulation of dorsal–intermediate lateral septum GABAergic neurons or dorsal–intermediate lateral septum GABAergic neurons to ventral tegmental area projections, the mice were implanted with optical fiber ferrules (diameter: 200 μm, length: 3.0 mm, numerical aperture: 0.48; Newson) into the dorsal–intermediate lateral septum bilaterally (coordinates, bregma: anterior–posterior: +0.5 mm; mediolateral: ±1.0 mm; dorsal–ventral: −3.0 mm, 18-degree angle), the ventral tegmental area received the dorsal–intermediate lateral septum output projections, or the fiber ferrules (diameter: 200 μm, length: 4.5 mm, numerical aperture: 0.48; Newson) were bilaterally implanted in the ventral tegmental area (coordinates, bregma: anterior–posterior: −3.2 mm; mediolateral: ±1.05 mm; dorsal–ventral: −4.4 mm, 7-degree angle). The optical fibers were secured using dental cement and skull screws. After surgery, the mice were housed individually to enable full recovery.

Polygraphic Recordings and Analysis

All sleep–wake state and anesthesia behavior experimental procedures took place between 9 AM and 7 PM (lights on at 7 AM). After 3 to 4 weeks for postoperative recovery and virus expression, the animals were housed individually in recording chambers and connected to the EEG/EMG head stages. The recording cable was attached to a slip-ring unit so that the movement of the mice would not be restricted. The mice were habituated to recording cables for 3 to 4 days before recording. EEG/EMG signals were recorded under baseline (free moving) and different treatment conditions (chemogenetic or optogenetic stimulations) over several days. For chemogenetic experiments, all mice received saline or clozapine *N*-oxide (1 mg/kg; HY-17366, MCE, USA) treatment at 10 AM (inactive period) before EEG/EMG recording for 2 h. To determine the effects of chemogenetic activation of the dorsal–intermediate lateral septum on power spectra for sleep–awake states, EEG power spectra were analyzed during the 2 h after clozapine *N*-oxide or saline injection. EEG and EMG signals derived from the surgically implanted electrodes were amplified × 1,000 (Pinnacle Technology, USA) and digitized at 400 Hz using sleep recording software (Pinnacle Technology). The signals were digitally filtered (EEG: 0.5 to 45 Hz, EMG: 50 to 200 Hz) and spectrally analyzed using fast Fourier transformation. Using sleep analysis software (SleepSign for animals, Kissei Comtec, Japan), the polygraphic recording signal was automatically analyzed based on spectral signatures of EEG/EMG waveforms. The recordings were first scored semiautomatically by 4-s epochs for the awake, non-REM sleep, and REM sleep states. The scoring was inspected visually based on the EEG/EMG waveforms and power spectra and corrected when appropriate. Wakefulness was defined as desynchronized low-amplitude EEG and heightened tonic EMG activity with phasic bursts. Non-REM sleep was defined as synchronized, high-amplitude, low-frequency (0.5 to 4 Hz) EEG and substantially reduced EMG activity compared with wakefulness, with no phasic bursts. REM sleep was defined as a pronounced theta rhythm (4 to 9 Hz) with no EMG activity. State transitions were identified when EEG/EMG criterion change was predominant for more than 50% of the epoch duration (*i.e.*, more than 2 s).

Optogenetic Stimulation during Polygraphic Recordings

After implantation of EEG/EMG electrodes and optical fibers, the mice were connected to an EEG/EMG recording cable and optical cables (1 m long, 200 μm in diameter; Thorlabs, USA) and allowed to habituate to the cables for at least 3 days. The joint was connected *via* a fiber to a 473-nm blue or 589-nm yellow laser diode (Newdoon). Light pulse trains were generated *via* a stimulator (SEN-7103, Nihon Kohden, Japan) and output through an isolator (ss-102J, Nihon Kohden). The intensity of the laser was tested using an optical power meter (PM100D, Thorlabs) and calibrated to 2 to 3 mW at the tip. To optogenetically stimulate the dorsal–intermediate lateral septum GABAergic neurons, pulses of 473-nm light (10 ms wide at 20 Hz) were delivered during non-REM or REM sleep to promote waking, whereas pulses of 589-nm light (10 ms wide at 20 Hz) were delivered in the awake state to promote non-REM–like sleep state. The EEG/EMG signal was visually monitored

in real time. Blue optical stimulation was applied after the onset of stable non-REM or REM sleep for 30 s at intervals of 10 to 15 min, and yellow optical stimulation was initiated in a stable state of wakefulness for 120 s at intervals of 20 to 30 min.

General Anesthesia Experiments

A subset of mice used in direct GABAergic optogenetic activation or inactivation experiments were utilized in the general anesthesia experiments. The mice were placed in an airtight acrylic chamber connected to an isoflurane vaporizer (RWD) and an isoflurane back absorption system (RWD). Baseline EEG/EMG in the awake state was recorded for 5 min. The mice were initially anesthetized using 2% isoflurane in 98% oxygen (2 l/min), and then 1.5% isoflurane was continuously delivered after the induction. A heating pad was used to maintain the body temperature at 35 to 37°C. The induction of anesthesia was behaviorally characterized as the loss of the righting reflex. Then 10 min after entering the stable burst suppression mode, 20-Hz optical activation lasting 60 s or optogenetic inhibition lasting 120 s was delivered. For the emergence from general anesthesia experiments, the mice were anesthetized for 30 min before the discontinuation of isoflurane administration. Once the isoflurane delivery was stopped, sustained optical stimulation (20-Hz pulse for 10 ms wide, 2 to 3 mW) was delivered until the righting reflex was restored. A common method for the quantification of burst suppression was used. First, we calculated the EEG voltage amplitude. According to the voltage threshold, the EEG was segmented into separate burst and suppression events. The voltage threshold was set according to the amplitude of the suppression waves of each mouse. If the EEG amplitude was less than their threshold, it was considered a suppression event with a score of 1; if the EEG amplitude was greater than the interval threshold, it was considered a burst event with a score of 0. EEG was shown as a binary time series. In this study, the minimum length of burst and suppression periods were set to 0.5 s, and the burst suppression ratio was calculated as the percentage of time spent in the suppression of each 30-s binary series.

EEG Spectral Analysis

The power spectra were computed using MATLAB (MathWorks, USA) and the Chronux signal processing toolbox (http://chronux.org/; accessed April 6, 2019). Signals were digitally low-pass filtered with a 45-Hz cutoff frequency using a third-order Butterworth filter and spectrally analyzed using the mtspectrumc function to provide information regarding the frequency, time, and amplitude of the EEG signals using Chronux2.12. The function parameter settings are as follows: window length, 2 s with 50% overlap; time-bandwidth product, 5; number of tapers, 9. The mean spectral density of all stimulated events per animal was sorted into successive 0.35-Hz frequency bands between 0 and 45 Hz. Then each frequency band was normalized to the sum of the power over the entire range (0 to 45 Hz). Frequency EEG bands were defined as delta (0.5 to 4 Hz), theta (4 to 9 Hz), alpha (9 to 12 Hz), spindle (12 to 18 Hz), beta (18 to 25 Hz), and gamma (25 to 45 Hz). Thereafter, we averaged each band power spectrum over time.

Fiber Photometry

Fluorescence emissions were recorded using a fiber photometry system (Thinkerbiotech, China). Briefly, the beam from a 488-nm laser (OBIS 488LS; Coherent) was reflected by a dichroic mirror (MD498; Thorlabs), focused by an ×10 objective lens (numerical aperture: 0.3; Olympus, Japan), and then coupled to an optical commutator (Doric Lenses, Canada). An optical fiber (optical density: 200 μm, numerical aperture: 0.48, 1 m long) guided the light between the commutator and the implanted optical fiber. The laser power at the tip of the optical fiber was adjusted to 40 to 60 μW. GCaMP6s fluorescence emission was bandpass filtered (MF525-39, Thorlabs) and collected using a photomultiplier tube (R3896, Hamamatsu, Japan). An amplifier (C7319, Hamamatsu) was used to convert the photomultiplier tube current output to voltage signals, which was further filtered through a low-pass filter (35-Hz cutoff; Brownlee 440). The analog voltage signals were amplified, digitized, and recorded at 100 Hz based on custom-written software in LabVIEW 2012 (National Instruments, USA). Analysis of the resulting signal was performed using custom written MATLAB software.

Fiber Photometry Data Analysis

Photometry data were exported to MATLAB for further analysis. We derived the value of the photometry signal ($\Delta F/F$) by calculating $(F - F_0)/F_0$, where F_0 is the baseline fluorescence signal. For the sleep–wake analysis, we recorded data for 4 to 6 h per mouse, including at least five transitions between different states, and calculated the averaged $\Delta F/F$ during all states for each mouse. To analyze the state transitions, we determined each state transition and aligned $\Delta F/F$ in a ±30-s window that was calculated around that point. For anesthesia state analysis, we recorded continuous changes in calcium signals from the awake state to anesthesia for each mouse under 1.5% isoflurane anesthesia for 1,200 s. According to the EEG/EMG data, we distinguished the calcium signals under different conditions (awake, anesthesia, and anesthesia recovery states) and then calculated the mean photometry signal under different conditions for each mouse.

Immunohistochemistry

The mice were deeply anesthetized using 2.0% isoflurane and perfused transcardially with 20 ml of phosphate-buffered saline, followed by 20 ml of ice-cold 4% paraformaldehyde in phosphate-buffered saline. The brains were carefully extracted from the skull and postfixed in 4% paraformaldehyde for 6 h and then dehydrated with 30% sucrose at 4°C until the brain

tissue sank to the bottom of the solution. Then 30-μm-thick coronal sections were cut using a freezing microtome (CM 3050S, Leica Microsystems, Germany). Free-floating sections were washed three times in phosphate-buffered saline for 10 min and blocked by incubation in phosphate-buffered saline with 1% bovine serum albumin (V900933-100G, Sigma–Aldrich, USA) and 0.1% Triton X-100 for 1 h. Sections were incubated with primary antibody diluted in phosphate-buffered saline and 0.1% Triton X-100 overnight at 4°C in a shaker. The primary antibodies used were rabbit anti–immediate early gene expression of proteins (c-Fos) (1:1,000; ABE457, Cell Signaling Technology, USA), mouse anti–glutamic acid decarboxylase 67 (GAD-67) (1:1,000; ab26116, Abcam, United Kingdom), mouse anti–tyrosine hydroxylase (1:1,000; MAB318, Millipore, USA), and mouse anti–calcium/calmodulin-dependent protein kinase IIα (1:200; catalog no. 50049, Cell Signal Technology, USA). Incubated slices were washed three times in phosphate-buffered saline for 10 min and incubated for 2 h with a secondary antibody in phosphate-buffered saline. The secondary antibodies used were Alexa Fluor 594 donkey anti-rabbit or Alexa Fluor 488 donkey anti-mouse (1:400; Invitrogen, USA). The samples were subsequently washed four times in phosphate-buffered saline for 10 min (all at room temperature); confocal images were acquired using the LSM 880 confocal microscope (Carl Zeiss, Germany) and further processed using ZEN 2.3 (blue edition) software (Zeiss).

In Vivo Electrophysiology Recordings

Adult *Vgat-Cre* mice were injected (200 μl/site) with recombinant AAV-Ef1α-DIO-ChR2-eYFP, AAV-Ef1α-DIO-NpHR-eYFP, or AAV-Ef1α-DIO-hM3Dq-mCherry into the dorsal–intermediate lateral septum bilaterally as described above. Recordings were performed at least 3 weeks after injection. The mice were anesthetized using 2% isoflurane and then maintained at 1.5% isoflurane on a stereotaxic apparatus. A heating pad was used to maintain the body temperature at 35 to 37°C. A single-channel optrode was constructed by assembling an optic fiber (numerical aperture: 0.48; Newdoon) parallel to a glass-coated tungsten electrode (1 to 3 MΩ; Alpha Omega Engineering, Israel). The vertical distance of the fiber to the tip of the electrode was approximately 100 to 200 μm. For constructing a single-channel injection electrode, a 200-μl pipette nozzle was burned and fused using an alcohol lamp to form a medium filament drug delivery pipeline, which was attached to the front of the electrode in parallel. The tip delivery port was approximately 100 to 200 μm from the tip of the electrode, and the other end of the drug delivery pipeline was connected to a microsyringe.

Photogenetic and Chemogenetic Verification Experiments

The skull window was opened at the top of the target brain region, and the position coordinates of the lateral septum were recorded (anterior–posterior: +0.5 mm, mediolateral: ± 0.4 mm, dorsal–ventral: −2.8 to −3.5 mm). The spikes were amplified ×20 using a differential amplifier, digitized (44 kHz), and stored using recording software from AlphaOmega SnR (Israel). When the spikes from visually responsive units were isolated, optical stimulation or clozapine *N*-oxide was administered for optogenetic or chemogenetic intervention to observe the effect of the intervention on neuron discharge.

Electrophysiologic Recording Experiments in the Ventral Tegmental Area

Craniotomies were performed (anterior–posterior: −3.2 to −3.5 mm, mediolateral: ±0.5 mm), and the optrodes were lowered into the ventral tegmental area (4.0 to 4.5 mm) through a guiding tube using a micromanipulator (AlphaOmega SnR). The spikes were amplified ×1,000 using a differential amplifier, digitized (44 kHz), and stored using the AlphaOmega recording software. When spikes from visually responsive units were isolated, light for optogenetic stimulation was generated using a 473-nm laser (frequency: 20 Hz; width: 10 ms; duration: 10 s; Newdoon); stimulus intensities, measured at the output of the optrode, ranged from 2 to 3 mW. The recording files were converted from the.mpx format to the .mat format using the Map/Mpx File Converter software (AlphaOmega SnR, version 5.1.8). All recorded neurons were sorted offline using principle component analysis in MATLAB to extract and represent the first two principal components on a two-dimensional plot of detected spike events. Waveforms with similar principal components were clustered using the *K*-means sorting method. An isolated cluster was considered as the same type of neurons. Unclassified neurons were discarded. Single putative dopaminergic neurons were also isolated and identified according to the following waveform and discharge characterizations: (1) action potential with triphasic waveform 2.0 ms in duration; (2) 1.1 ms from spike onset to negative trough; and (3) slow spontaneous firing rate of less than 10 spikes/s.[22] GABAergic neurons in the ventral tegmental area were distinguished from dopaminergic neurons based on their relatively high rapid-firing, nonbursting activity and short-duration action potentials (less than 0.5 ms).[23,24] There was another group of neurons whose waveforms were different from those of dopaminergic and GABAergic neurons, and we designated them as glutamatergic neurons. Three types of neurons were classified; they were calculated by counting the number of spikes that occurred within 10 s after stimulus onset and subtracting this by the number of spikes that would have occurred had the firing rate remained the same as that seen during baseline (calculated as the average firing rate for 10 s before stimulus onset). Firing rates were calculated from the peristimulus time histogram using bins of 0.25 s.

Statistical Analysis

The parametric data are expressed as the means ± SD, and nonparametric data are presented as medians (25th, 75th percentiles); outliers, if any, were always included in the analyses. Sample sizes were determined based on previous publications on sleep–wake state regulation using chemogenetic and optogenetic approaches. No *a priori* statistical power calculation was conducted. Parametric tests were used if the data set passed the assumptions required for parametric analysis including level of measurement, normality, and homogeneity of variances. Otherwise, nonparametric tests were used. We used paired or independent unpaired two-tailed Student's *t* tests for comparisons between two groups satisfied parameter analysis. The Mann–Whitney rank sum test or Wilcoxon signed rank test was used when at least one variable violated the assumptions required for parametric analysis. One-way ANOVA followed by Tukey's *post hoc* analysis was used for comparing three or more groups. All statistical analyses were performed using SPSS 13.0. or MATLAB if necessary. Significant differences were set at $P < 0.05$.

Results

GABAergic Neurons in Dorsal–Intermediate Lateral Septum Are Activated in Awake State

c-Fos, expressed by an immediate early gene, is generally used as a marker for activated neurons.[25] To observe the neuronal activities, we first detected the c-Fos expressions in the lateral septum during wakefulness, sleep, and different anesthesia states (fig. 1, A and B). There were higher levels of c-Fos expressions in the dorsal–intermediate lateral septum at 8 PM and after extended wakefulness (at 10 PM), as compared to at 8 AM or at 10 AM (8 AM *vs.* 8 PM: 56 ± 15 c-Fos$^+$ cells/mm^2 *vs.* 109 ± 17 c-Fos$^+$ cells/mm^2, $P < 0.001$; 8 AM *vs.* 10 PM: 56 ± 15 c-Fos$^+$ cells/mm^2 *vs.* 91 ± 11 c-Fos$^+$ cells/mm^2, $P < 0.001$; 10 AM *vs.* 8 PM: 57 ± 12 c-Fos$^+$ cells/mm^2 *vs.* 109 ± 17 c-Fos$^+$ cells/mm^2, $P < 0.001$; and 10 AM *vs.* 10 PM: 57 ± 12 c-Fos$^+$ cells/mm^2 *vs.* 91 ± 11 c-Fos$^+$ cells/mm^2, $P < 0.001$, n = 9 slices from 3 mice/group; fig. 1, B and C). Compared with that in the awake state (10 PM), the expressions of c-Fos were significantly decreased in different anesthesia states (wake *vs.* induction: 113 ± 18 c-Fos$^+$ cells/mm^2 *vs.* 62 ± 17 c-Fos$^+$ cells/mm^2, $P < 0.001$; wake *vs.* maintenance: 113 ± 18 c-Fos$^+$ cells/mm^2 *vs.* 35 ± 10 c-Fos$^+$ cells/mm^2, $P < 0.001$; emergence *vs.* induction: 86 ± 17 c-Fos$^+$ cells/mm^2 *vs.* 62 ± 17 c-Fos$^+$ cells/mm^2, $P = 0.017$; emergence *vs.* maintenance: 86 ± 17 c-Fos$^+$ cells/mm^2 *vs.* 35 ± 10 c-Fos$^+$ cells/mm^2, $P < 0.001$, n = 9 slices from 3 mice/group; fig. 1, B and D). Due to c-Fos immunofluorescence, the studies were done in the absence of EEG/EMG to confirm arousal state scoring. To directly examine the dynamic activities of dorsal–intermediate lateral septum neurons *in vivo* across spontaneous sleep–wakefulness and different anesthesia states, we employed fiber photometry to detect the calcium signals of the dorsal–intermediate lateral septum GABAergic neurons in freely moving mice. After stereotaxic injection of the Cre-dependent AAV vector encoding the fluorescent calcium indicator GCaMP6s (AAV-Ef1α-DIO-GCaMP6s) into the right dorsal–intermediate lateral septum of *Vgat-Cre* mice, we implanted the mice with fiber optic probes for subsequent delivery of excitation light and collection of fluorescent emission, in combination with EEG-EMG electrodes for simultaneous and continuous recordings in sleep–wake and different anesthesia states (fig. 1E). Immunofluorescence staining results showed that 93% GCaMP6s-expressing cells were glutamic acid decarboxylase 67 (GAD-67)–positive (fig. 1F), suggesting that they are mainly GABAergic neurons. When comparing the fluorescence signals of the GABAergic neurons in the dorsal–intermediate lateral septum, we found robust alterations across arousal states. During non-REM sleep, dorsal–intermediate lateral septum GABAergic neurons showed lower fluorescence signals than those during either awake or REM sleep states (wake *vs.* non-REM sleep: 3.3 ± 1.4% *vs.* –1.3 ± 1.2%, $P < 0.001$; REM sleep *vs.* non-REM sleep: 5.3 ± 1.3% *vs.* –1.3 ± 1.2%, $P < 0.001$, n = 7 mice/group; fig. 1, G and H; Supplemental Digital Content 1, fig. 1A, http://links.lww.com/ALN/C642). Notably, the activities of the dorsal–intermediate lateral septum GABAergic neurons decreased before awake–to–non-REM sleep (0.7 ± 0.3% *vs.* –0.4 ± 0.3%, $P < 0.001$, n = 7 mice/group) and REM sleep-to-awake transitions (–0.2 ± 0.7% *vs.* –0.6 ± 1.0%, $P = 0.016$, n = 7 mice/group) and increased before non-REM sleep-to-REM sleep (0.2 ± 0.3% *vs.* 1.4 ± 0.6%, $P < 0.001$, n = 7 mice/group) and non-REM sleep-to-awake transitions (0.2 ± 0.3% *vs.* 1.2 ± 0.7%, $P = 0.003$, n = 7 mice/group; Supplemental Digital Content 1, fig. 2, http://links.lww.com/ALN/C642). In contrast, the dorsal–intermediate lateral septum GABAergic neurons showed higher fluorescence signals during REM sleep than those during either awake or non-REM sleep states (fig. 1, G and H). With deepening anesthesia, the fluorescence signals of dorsal–intermediate lateral septum GABAergic neurons became weak and then gradually recovered as the isoflurane anesthesia stopped (preanesthesia *vs.* anesthesia: 2.6 ± 1.2% *vs.* –1.3 ± 0.8%, $P < 0.001$; anesthesia *vs.* post anesthesia: –1.3 ± 0.8% *vs.* 0.2 ± 1.2%, $P = 0.046$, n = 7 mice/group; fig. 1, I and J; Supplemental Digital Content 1, fig. 1B, http://links.lww.com/ALN/C642). These findings demonstrate that the dorsal–intermediate lateral septum GABAergic neurons change their activities across sleep–awake and different anesthesia states, suggesting the involvement of the dorsal–intermediate lateral septum GABAergic neurons in regulating sleep–awake and anesthesia states.

Chemogenetic Activation of Dorsal–Intermediate Lateral Septum GABAergic Neurons Increase Wakefulness

We next determined the necessity of dorsal–intermediate lateral septum activities for wakefulness by activating the

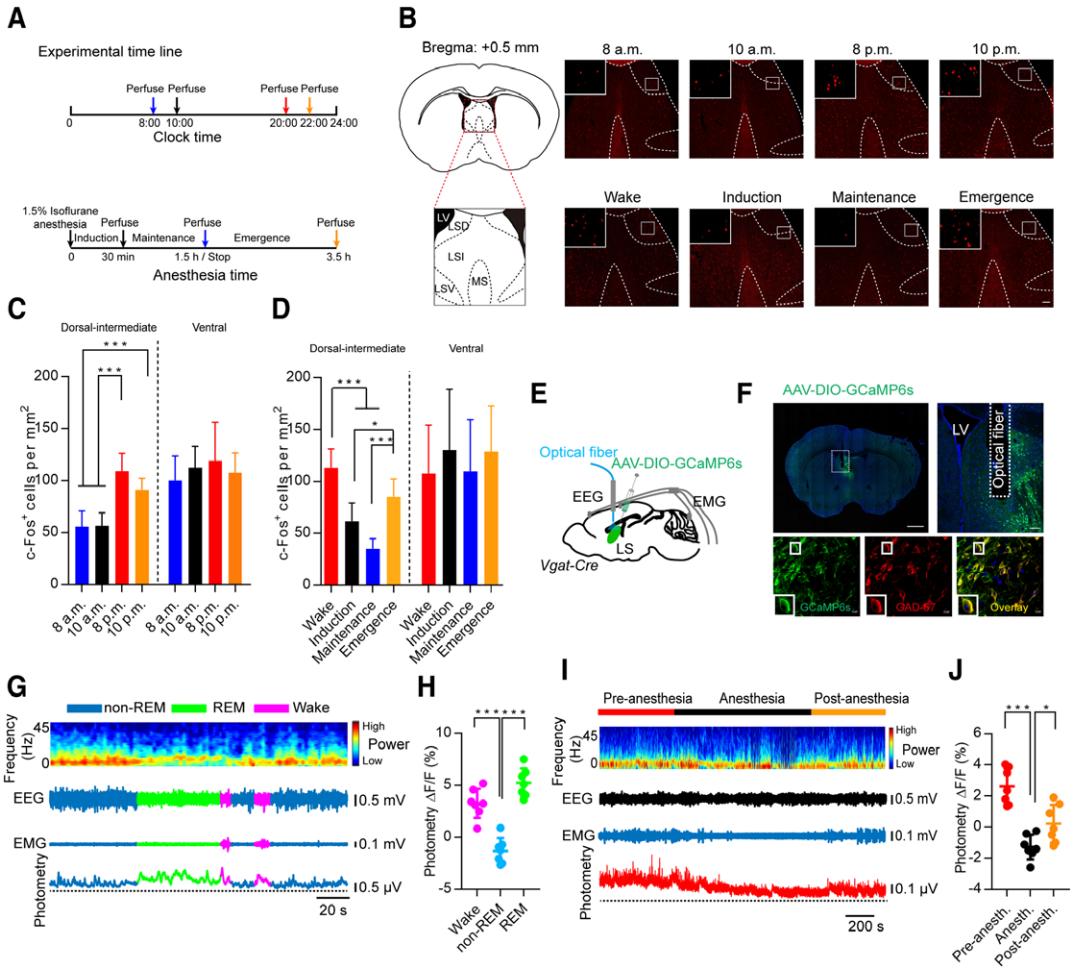

Fig. 1. Activities of the dorsal–intermediate lateral septum (LS) γ-aminobutyric acid–mediated neurons across sleep–awake states. (*A*) Timeline of immediate early gene expression of proteins (c-Fos) staining during sleep–wake and different anesthesia states. (*B*) *Top*: Coronal images showing c-Fos expression in the lateral septum at the sleep stage. *Bottom*: Coronal images showing c-Fos expression in the lateral septum during different periods of anesthesia. *Scale bar*, 100 μm. (*C*) The c-Fos expression in dorsal–intermediate lateral septum (n = 9 slices from 3 mice/group, one-way ANOVA followed by Tukey's *post hoc* test: $F_{3,32} = 31.34$, $P < 0.001$; *P* [8 am to 8 pm] < 0.001, *P* [8 am to 10 pm] < 0.001, *P* [10 am to 8 pm] < 0.001, *P* [10 am to 10 pm] < 0.001), and ventral lateral septum (LSV; n = 9 slices from 3 mice/group, one-way ANOVA: $F_{3,32} = 0.89$, $P = 0.457$). (*D*) With the deepening of anesthesia, the expression of c-Fos gradually decreased and gradually recovered in dorsal–intermediate lateral septum (n = 9 slices from 3 mice/group, one-way ANOVA followed by Tukey's *post hoc* test: $F_{3,32} = 39.21$, $P < 0.001$; *P* [wake-induction] < 0.001, *P* [wake-maintenance] < 0.001, *P* [induction-emergence] = 0.017, *P* [maintenance-emergence] < 0.001) after the cessation of anesthesia. However, c-Fos expression of ventral lateral septum (n = 9 slices from 3 mice/group, one-way ANOVA: $F_{3,32} = 0.52$, $P = 0.669$) did not change under different anesthesia periods. (*E*) Schematic of the virus injection, fiber photometry setup, and *in vivo* electroencephalogram (EEG)/electromyography (EMG) recording configuration. (*F*) *Top left*: Unilateral viral targeting of adeno-associated virus (AAV)-DIO-GCaMP6s into the lateral septum. *Scale bar*, 1,000 μm. *Top right*: Location of the optical fiber in the dorsal–intermediate lateral septum. *Scale bar*, 100 μm. *Bottom row*: Magnified image showing the expression of GCaMP6s-positive (*green*) and glutamic acid decarboxylase 67 (GAD-67) (*red*) cells and the co-expression of GAD-67 (*red*) in GCaMP6s-positive (*green*) cells. *Scale bar*, 10 μm. (*G*) Representative fluorescence traces, relative EEG power spectra, and EEG/EMG traces across spontaneous sleep–wakefulness states. Voltage represents the change in fluorescence for the entire time series. (*H*) Statistics for the fluorescence signals during the awake state, non–rapid eye movement (non-REM) sleep, and REM sleep (each dot represents the average for each mouse, n = 7 mice, 5 sessions per mouse, one-way ANOVA followed by Tukey's *post hoc* test: $F_{2,18} = 43.72$, $P < 0.001$; *P* [non-REM–awake state] < 0.001, [non-REM–REM] < 0.001). (*I*) Sample EEG power spectrum, EEG-EMG traces, and raw fluorescence trace in a continuous anesthesia state from the awake state to the anesthesia induction period, deep anesthesia, and anesthesia recovery period. (*J*) Summary of fluorescence signals during preanesthesia (Pre-anesth.), anesthesia (Anesth.), and postanesthesia (Post. anesth.) (each *dot* represents the average for each mouse, n = 7 mice, 5 sessions per mouse, one-way ANOVA followed by Tukey's post hoc test; $F_{2,18} = 23.28$, $P < 0.001$; *P* [preanesthesia-anesthesia] < 0.001, *P* [anesthesia-postanesthesia] = 0.046). The data represent means ± SD. **P* < 0.05; ****P* < 0.001. LSD, dorsal lateral septum; LSI, intermediate lateral septum; LV, lateral ventricle; MS, medial septum.

dorsal–intermediate lateral septum GABAergic neurons chemogenetically *via* bilaterally injecting an AAV virus encoding the engineered Gq-coupled hM3D receptor (AAV-Ef1α-DIO-hM3Dq-mCherry) into the dorsal–intermediate lateral septum of *Vgat-Cre* mice (fig. 2, A and B). *In vivo* electrophysiology recordings of the dorsal–intermediate lateral septum GABAergic neurons confirmed that clozapine *N*-oxide (5 μ M, 1 μl) potently activated the hM3D-expressing dorsal–intermediate lateral septum neurons (fig. 2C). Similarly, we implanted the mice with EEG/EMG electrodes for sleep–wakefulness monitoring and investigated the effect of dorsal–intermediate lateral septum GABAergic neurons activation in freely moving mice. Saline (0.1 ml) or clozapine *N*-oxide (1 mg/kg, 0.1 ml) was injected intraperitoneally into the mice at 10 AM (3 h after lights on), a period when mice usually show a high level of spontaneous sleep, which is characterized by a typical light-phase hypnogram with long bouts of non-REM sleep marked by the high EEG delta power and low EMG activity. Clozapine *N*-oxide significantly increased wakefulness (saline *vs*. clozapine *N*-oxide: 41.4 ± 19.2 min *vs.* 82.0 ± 18.8 min, $P = 0.001$, n = 7 mice/group), with decreased non-REM sleep (saline *vs*. clozapine *N*-oxide: 77.7 ± 18.5 min *vs.* 37.9 ± 17.3 min, $P = 0.001$, n = 7 mice/group) during the 2 h after administration as compared with saline. During the 2 h post-injection period, clozapine *N*-oxide administration resulted in a 100.5% increase in wakefulness and a 51.2% reduction in non-REM sleep (fig. 2, D and E).

Optogenetic Activation of Dorsal–Intermediate Lateral Septum GABAergic Neurons Initiates Wakefulness and Accelerates Anesthesia Emergence

Because optogenetics modulates neuronal activities at a millisecond time scale,[26] we used it to examine the capacity of dorsal–intermediate lateral septum GABAergic neurons to initiate wakefulness. To genetically target GABAergic neurons in the dorsal–intermediate lateral septum area, we stereotactically injected a Cre-inducible AAV vector encoding either eYFP (control) or the light-activatable ChR2 fused to eYFP (ChR2-eYFP) bilaterally into *Vgat-Cre* mice, along with bilateral optical fiber implantation for illumination with blue laser light and electrodes for EEG/EMG recording (fig. 3, A and B). Electrophysiologic recordings *in vivo* confirmed the function of ChR2 (fig. 3C). We also applied optical stimulation (lasting 30 s) after the onset of stable non-REM sleep during the light phase. Optical stimulation of the dorsal–intermediate lateral septum GABAergic neurons during non-REM sleep reliably induced transitions to the awake state (fig. 3D; Supplemental Digital Content 2, http://links.lww.com/ALN/C643). Optical stimulation of the dorsal–intermediate lateral septum for a shorter duration (within 1 to 5 s of light pulse onset) was still sufficient to induce such transitions, which were characterized by EEG desynchronization, EMG activation, and behavioral wakefulness in ChR2-eYFP mice (153.0 [115.9, 179.7] s *vs.* 4.0 [3.4, 4.6] s, $P = 0.009$, n = 5 mice/group; fig. 3E). Spectrum analysis indicated that optical stimulation resulted in an overt increase in wakefulness, with an increase in theta, beta, and gamma power (theta: 25.7 ± 4.5% *vs.* 37.7 ± 3.8%, $P = 0.002$; beta: 4.3 [4.0, 7.1] % *vs.* 24.0 [18.9, 25.6] %, $P = 0.009$; gamma: 6.7 [4.9, 9.5] % *vs.* 9.0 [9.1, 18.0] %, $P = 0.117$, n = 5 mice/group; fig. 3, F through I). In contrast, photostimulation during REM sleep exerted no effect on sleep–wake or EEG/EMG activity in ChR2-eYFP mice. The mice remained undisturbed and REM sleep continued during the entire stimulation period (latency to wake: 104.8 ± 40.9 s *vs.* 100.8 ± 43.9, $P = 0.885$; delta: 15.5 ± 4.7% *vs.*14.1 ± 4.3%, $P = 0.645$; theta: 40.7 ± 16.2% *vs.* 43.5 ± 17.8%, $P = 0.801$; beta: 7.7 ± 4.4% *vs.* 7.7 ± 4.3%, $P = 0.975$; gamma: 7.1 [5.0, 24.0] % *vs.* 7.2 [4.4, 23.5] %, $P = 0.917$, n = 5 mice/group; Supplemental Digital Content 1, fig. 3, A through D, http://links.lww.com/ALN/C642). These findings demonstrate that activation of the dorsal–intermediate lateral septum GABAergic neurons rapidly triggered non-REM–awake but not REM–awake transitions.

We next investigated whether the activation of GABAergic neurons is sufficient to induce wakefulness from an unconscious state under general anesthesia induced by isoflurane. When stable EEG burst-suppression mode, a marker of anesthetic depth, was observed, 20-Hz stimulation (lasting 60 s) caused an immediate increase in total EEG burst activity. This increase in burst activity was accompanied by an increase in number of bursts, a prolonged burst duration, and a decreased burst suppression ratio (number of bursts: 9.0 [8.4, 9.3] *vs.* 14.0 [12.1, 14.9], $P = 0.001$; burst duration: 2.7 ± 0.6 s *vs.* 3.9 ± 0.7 s, $P = 0.003$; burst suppression ratio: 63.1 ± 11.4% *vs.* 15.7 ± 9.4%, $P < 0.001$, n = 8 mice/group; fig. 3, J through M) in ChR2-eYFP group mice. Additionally, sustained activation of dorsal–intermediate lateral septum GABAergic neurons significantly accelerated the emergence from isoflurane-induced unconsciousness (514.4 ± 122.2 s *vs.* 226.5 ± 53.3 s, $P < 0.001$, n = 8 mice/group; fig. 3N).

Silencing of Dorsal–Intermediate Lateral Septum GABAergic Neurons Induces Non-REM–like Sleep State and Prolongs Emergence Time

To test whether silencing of dorsal–intermediate lateral septum GABAergic cells promote non-REM sleep, we transduced the dorsal–intermediate lateral septum of *Vgat-Cre* mice with AAV-DIO-NpHR-eYFP or AAV-DIO-eYFP and implanted bilateral optical fibers above the dorsal–intermediate lateral septum for *in vivo* optical silencing while recording cortical EEG and EMG signals (fig. 4, A and B). Using *in vivo* electrophysiologic recordings, we found that yellow illumination resulted in the inhibition of dorsal–intermediate lateral septum GABAergic neurons (fig. 4C). We also found that optogenetic silencing of dorsal–intermediate lateral septum GABAergic neurons

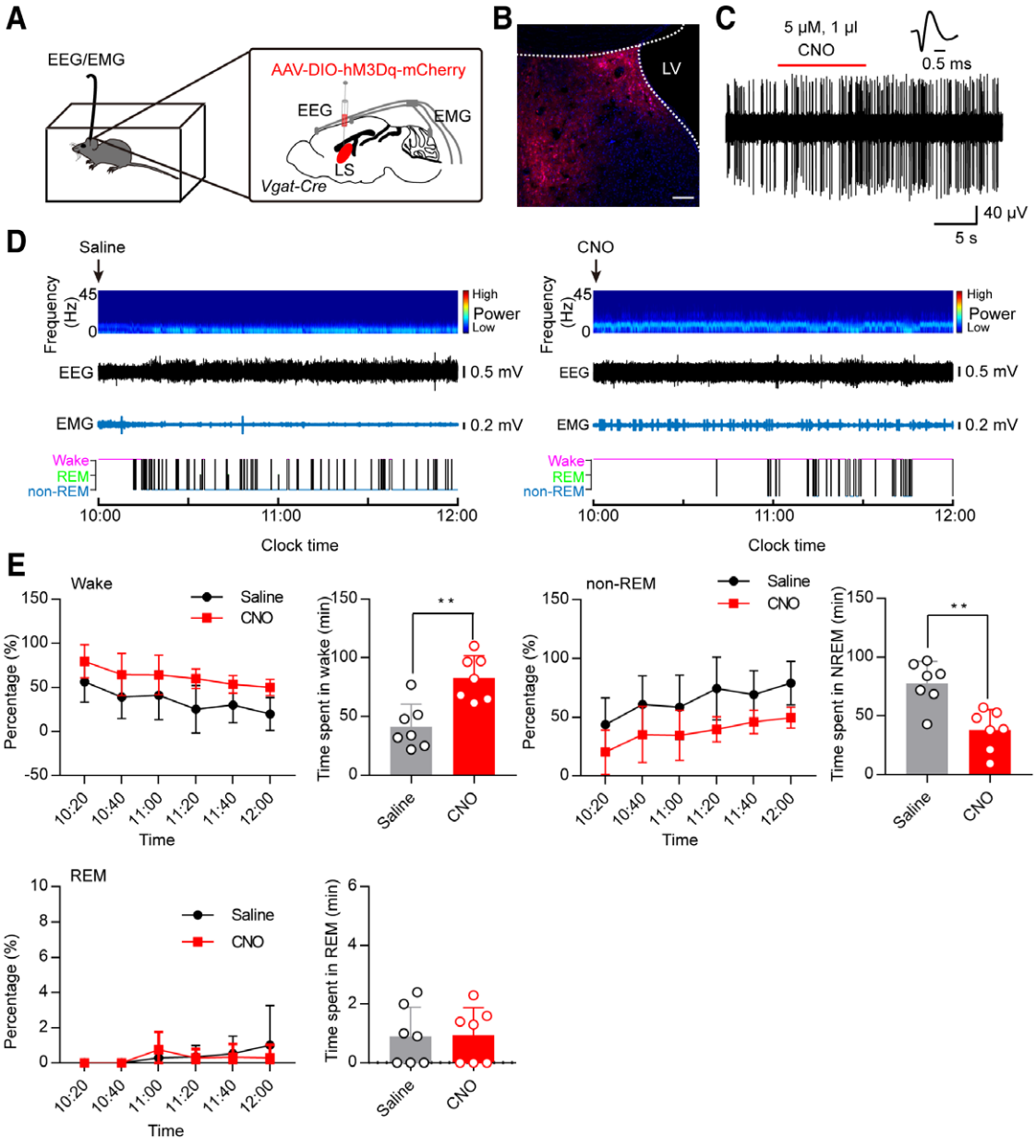

Fig. 2. Chemogenetic activation of the dorsal–intermediate lateral septum (LS) γ-aminobutyric acid–mediated (GABAergic) neurons enhanced the awake state and suppresses non–rapid eye movement (non-REM) sleep. (*A*) Schematic of virus injection and electroencephalogram (EEG)/electromyography (EMG) recordings. (*B*) Sample image showing the expression of hM3Dq-mCherry in dorsal–intermediate lateral septum neurons. *Scale bar*, 100 μm. (*C*) Representative voltage traces recorded from the mCherry-expressing neuron during clozapine *N*-oxide (CNO) administration. CNO significantly increased the firing frequencies in hM3Dq-positive GABAergic neurons in the dorsal–intermediate lateral septum. (*D*) Typical EEG/EMG traces and hypnograms during the 2 h after saline or CNO (1 mg/kg) injection at 10:00 am. (*E*) Time course changes in the awake state, non-REM sleep, and REM sleep after administration of saline or CNO to the mice with hM3Dq expressed in the dorsal–intermediate lateral septum GABAergic neurons. Summary data are shown for the total time spent in each stage for 2 h after saline or CNO injection. Unpaired two-tailed Student's *t* test: $t_{12} = 4.10$, $P = 0.001$ (awake state); $t_{12} = 4.16$, $P = 0.001$ (non-REM); $t_{12} = 0.08$, $P = 0.935$ (REM). The data represent means ± SD. $^{**}P < 0.01$.

during the awake state induced a non-REM–like sleep state (278.0 [221.0, 303.8] s *vs.* 40.0 [36.3, 47.5] s, $P < 0.001$, n = 7 mice/group; fig. 4D). However, the time from the awake state to the non-REM–like sleep state (within 28 to 58 s of light pulse onset; fig. 4E) was longer than the optogenetic activation time of dorsal–intermediate lateral septum

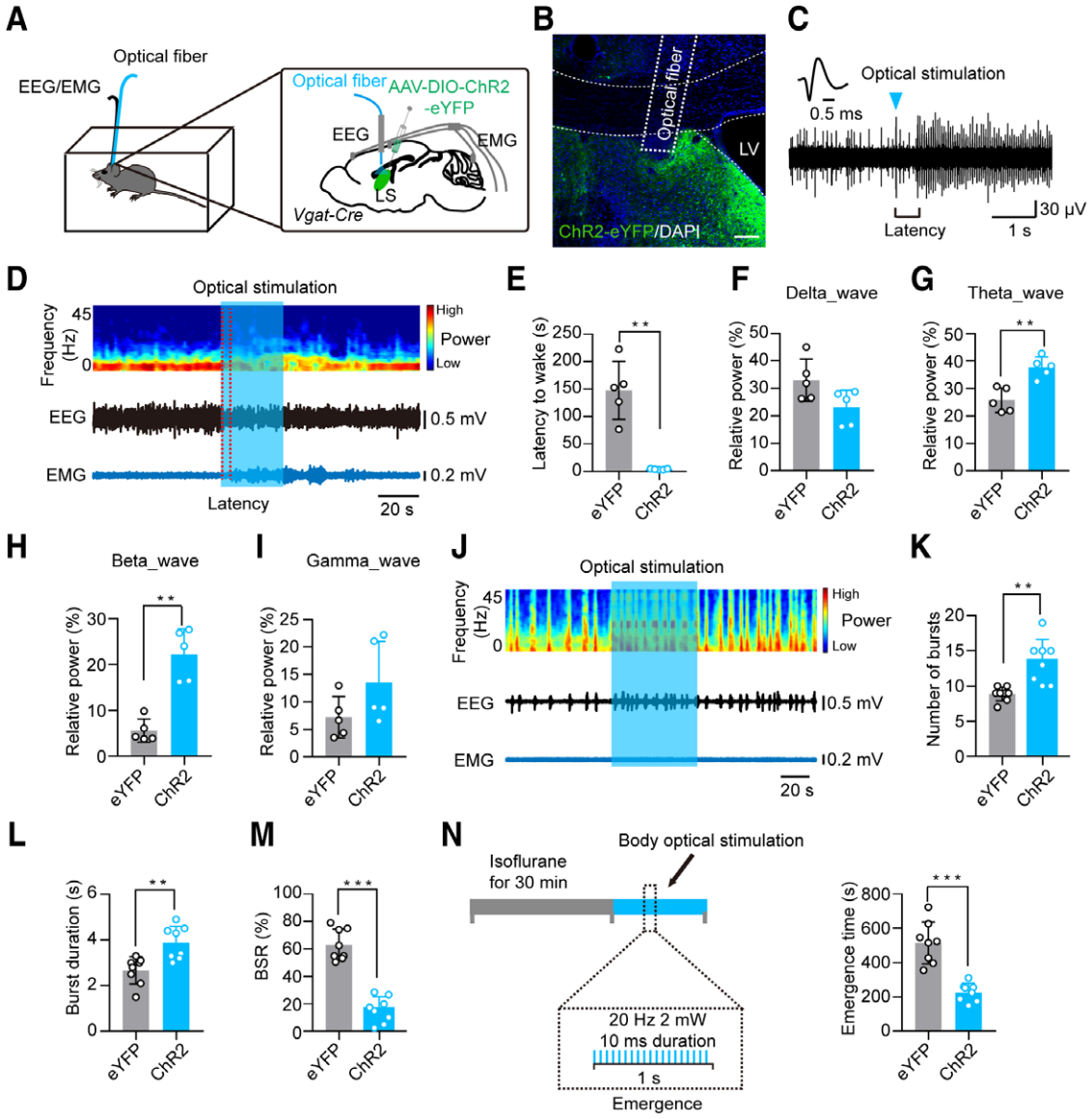

Fig. 3. Optogenetic activation of the dorsal–intermediate lateral septum (LS) γ-aminobutyric acid–mediated (GABAergic) neurons induced wakefulness from sleep and emergence from general anesthesia. (*A*) Schematic of optogenetic activation of the dorsal–intermediate lateral septum GABAergic neurons and electroencephalogram (EEG)/electromyography (EMG) recordings. (*B*) Representative image showing the channelrhodopsin-2 (ChR2)-enhanced yellow fluorescent protein (eYFP) expression and location of the optical fiber in the dorsal–intermediate lateral septum. *Scale bar*, 100 μm. (*C*) Example traces of firing changes of ChR2-expressing dorsal–intermediate lateral septum neurons evoked by 473-nm light stimulation with 20-Hz pulses. (*D*) Representative EEG/EMG traces and heat map of EEG power spectra showing that acute photostimulation (20 Hz/30 s) applied during non–rapid eye movement (non-REM) sleep induced a transition to the awake state in the ChR2-eYFP mouse. (*E*) Mean latencies of non-REM to sleep-to-awake transitions after optogenetic stimulation at 20 Hz: $P = 0.009$, $U = 0.00$; Mann–Whitney rank sum test (two-tailed). (*F* through *I*) Average of normalized relative cortical EEG delta, theta, beta, and gamma power (n = 5 mice/condition, average 5 episodes/animal). Delta: $t_8 = 2.24$, $P = 0.056$; theta: $t_8 = 4.54$, $P = 0.002$, unpaired two-tailed Student's *t* test; beta: $U = 0.00$ $P = 0.009$ and gamma: $U = 5.00$ $P = 0.117$, Mann–Whitney rank sum test (two-tailed). (*J*) Sample EEG power spectrum and EEG/EMG traces at approximately 20-Hz stimulation during isoflurane-induced general anesthesia. (*K* through *M*) Summary showing increased burst numbers and burst duration, as well as decreased burst suppression ratio (BSR) during periods of 20 Hz optical stimulation. Number of bursts: $U = 2.00$ $P = 0.001$, Mann–Whitney rank sum test (two-tailed); burst duration: $t_{14} = 3.64$, $P = 0.003$ and burst suppression ratio: $t_{14} = 9.09$, $P < 0.001$ unpaired two-tailed Student's *t* test. (*N*) *Left*: Schematic of the sustained optical stimulation protocol after the discontinuation of isoflurane administration. *Right*: Summary results showing that compared with the eYFP group, 20-Hz continuous optical stimulation significantly decreased the emergence time, $t_{14} = 6.11$, $P < 0.001$, unpaired two-tailed Student's *t* test. The data represent means ± SD. $^{**}P < 0.01$; $^{***}P < 0.001$. DAPI, 4′,6-diamidino-2-phenylindole; LV, lateral ventricle.

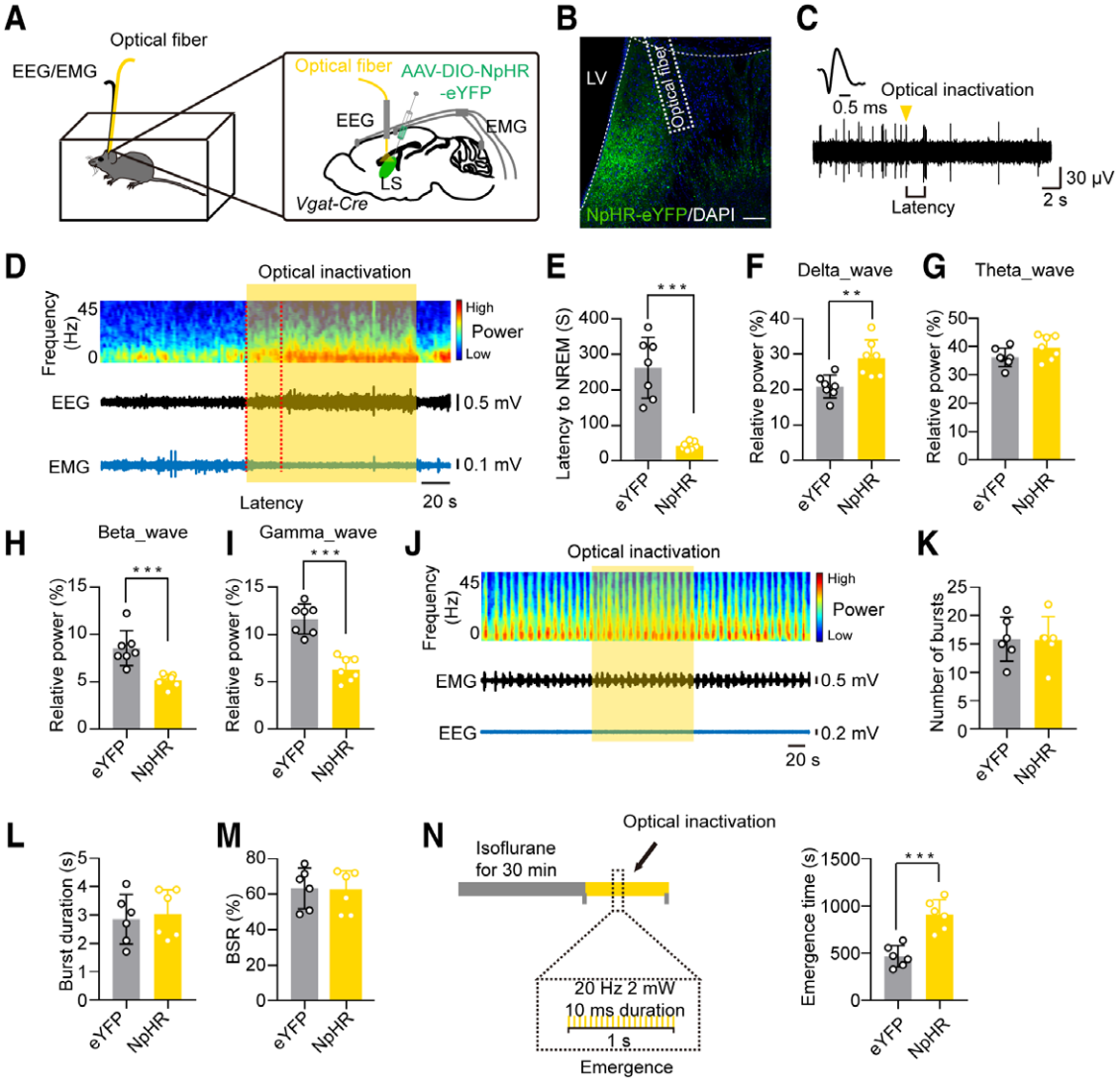

Fig. 4. Optogenetic inhibition of the dorsal–intermediate lateral septum (LS) γ-aminobutyric acid–mediated (GABAergic) neurons during the awake state promoted non–rapid eye movement (NREM)–like sleep state and prolonged emergence time. (*A*) Schematic of optogenetic inactivation of the dorsal–intermediate lateral septum GABAergic neurons and electroencephalogram (EEG)/electromyography (EMG) recordings. (*B*) Typical photomicrographs showing enhanced yellow fluorescent protein (eYFP)-labeled dorsal–intermediate lateral septum cells. *Scale bar*, 100 μm. (*C*) Example traces of firings showing that optical stimulation reliably inhibited the firing activities of NpHR-eYFP neurons. (*D*) Representative EEG/EMG traces and EEG heat map for NpHR-eYFP. Animals showing changes in EEG oscillation, EMG, and correspondent heat map EEG power spectrum in response to local optical silencing (yellow light stimulation, 593 nm) during the awake state. (*E*) Awake-to-sleep transitions after optogenetic stimulation at 20 Hz. $U = 0.00$, $P < 0.001$, Mann–Whitney rank sum test (two-tailed). (*F* through *I*) Summary showing increased normalized relative cortical EEG spectral delta power and decreased beta and gamma power. Unpaired two-tailed *t* test. Delta: $t_{12} = 3.47$, $P = 0.005$; theta: $t_{12} = 1.70$, $P = 0.114$; beta: $t_{12} = 4.55$, $P < 0.001$; gamma: $t_{12} = 6.99$, $P < 0.001$. (*J*) Representative EEG/EMG traces and heat map of EEG power spectra showing that acute photostimulation applied during the awake state induced a transition to non-REM sleep in the NpHR-eYFP mouse. (*K* through *M*) Summary data showing that burst numbers, burst duration, and burst suppression ratio (BSR) did not change during periods of 20-Hz optical stimulation. Unpaired two-tailed *t* test. Number of bursts: $t_{10} = 0.07$, $P = 0.944$; burst duration: $t_{10} = 0.37$, $P = 0.721$; burst suppression ratio: $t_{10} = 0.29$, $P = 0.780$. (*N*) *Left*: Diagram for optical stimulation and recording of emergence time. Laser stimulation was initiated after turning off isoflurane administration and ended with recovery of righting. *Right*: Summary showing that optical inactivation of dorsal–intermediate lateral septum GABAergic neurons prolonged emergence time from 1.5% isoflurane anesthesia. $t_{10} = 5.45$, $P < 0.001$, unpaired two-tailed Student's *t* test. The data represent means ± SD. $^{**}P < 0.01$; $^{***}P < 0.001$. DAPI, 4′,6-diamidino-2-phenylindole; LV, lateral ventricle.

GABAergic neurons to induce wakefulness (fig. 3, D and E), which means that the activation of dorsal–intermediate lateral septum GABAergic neurons induce arousal more easily than the inhibition of GABAergic neurons induce the non-REM–like sleep state. The following spectral analysis showed that the delta EEG power was increased and the beta and gamma powers were decreased upon dorsal–intermediate lateral septum GABAergic neuron inactivation (delta: 20.8 ± 3.2% *vs.* 28.9 ± 5.2%, $P = 0.005$; theta: 36.2 ± 3.3% *vs.* 39.7 ± 4.3%, $P = 0.114$; beta: 8.6 ± 1.9% *vs.* 5.2 ± 0.7%, $P < 0.001$; gamma: 11.7 ± 1.6% *vs.* 6.3 ± 1.3%, $P < 0.001$, n = 7 mice/group; fig. 4, F through I).

Furthermore, GABAergic neurons of the dorsal–intermediate lateral septum were optically inactivated once stable burst suppression was recorded from the cortex. Interestingly, a single 120-s bilateral optical inactivation did not cause a significant change in the burst activity in the cortex, including the number of bursts, the burst duration, and the burst suppression ratio (number of bursts: 15.8 ± 3.9 *vs.* 15.7 ± 4.1, $P = 0.944$; burst duration: 2.9 ± 0.9 s *vs.* 3.0 ± 0.9 s, $P = 0.721$; burst suppression ratio: 63.4 ± 11.5% *vs.* 61.5 ± 11.8%, $P = 0.780$, n = 6 mice/group; fig. 4, J through M). This supports that it is always more difficult to silence neurons than to depolarize them. In addition, when brain function is inhibited deeply by isoflurane, dorsal–intermediate lateral septum GABAergic neurons have a weak inhibitory effect on brain function. However, sustained inactivation of dorsal–intermediate lateral septum GABAergic neurons significantly prolonged the emergence from isoflurane-induced unconsciousness (466.3 ± 113.7 s *vs.* 905.0 ± 161.1 s, $P < 0.001$, n = 7 mice/group; fig. 4N).

Dorsal–Intermediate Lateral Septum Axons Form Monosynaptic GABAergic Synapses on Ventral Tegmental Area GABAergic Neurons

Recent studies have reported that the lateral septum is linked to positive reinforcement.[27,28] The lateral septum contains mainly GABAergic neurons and is a source of GABAergic input to the ventral tegmental area, which participates in sleep–wakefulness control.[15,29] Because the dorsal lateral septum stimulation activates a significant number of ventral tegmental area neurons, inhibition of ventral tegmental area GABAergic interneurons, through a GABA–GABA connection between the lateral septum and the ventral tegmental area, is responsible for the increased activities of ventral tegmental area dopaminergic neurons related to sleep–wakefulness regulation.[15,30] To test this, we used a potential novel anterograde monosynaptic tracer, the modified herpes simplex virus H129-ΔTK-tdT. With the helper virus AAV-Ef1α-DIO-EGFP-2a-TK-WPRE-pA complementarily expressing TK, H129-ΔTK-tdT transmits to postsynaptic neurons, enabling visualization of the monosynaptic output.[31] To trace the monosynaptic output of dorsal–intermediate lateral septum-GABA neurons, AAV-Ef1α-DIO-EGFP-2a-TK-WPRE-pA and H129-ΔTK-tdT were injected into the dorsal–intermediate lateral septum of *Vgat-Cre* mice on days 0 and 22, respectively (fig. 5, A and E). Sequentially, we observe a crowd of tdTomato-labeled neurons in the ventral tegmental area, suggesting that the dorsal–intermediate lateral septum GABAergic neurons monosynaptically innervated the ventral tegmental area neurons (fig. 5B).

In addition to dopaminergic neurons, the ventral tegmental area also contains GABAergic and glutamatergic neurons. It has been demonstrated that activating dopaminergic and glutamatergic/NOS1 neurons promotes wakefulness and REM sleep, whereas ventral tegmental area GABAergic neurons elicited long-lasting non-REM–like sleep resembling sedation.[8] To confirm the cell type of the dorsal–intermediate lateral septum-innervated ventral tegmental area neurons, we labeled the ventral tegmental area dopaminergic neurons with tyrosine hydroxylase, glutamatergic neurons with calcium/calmodulin-dependent protein kinase IIα (fig. 5C), and the GABAergic neurons by injecting the *Vgat-Cre*-dependent GABA-GFP into the ventral tegmental area (fig. 5, E and F). The following results suggested that 70.7% tdTomato-positive cells were GABAergic (fig. 5G), whereas only 17.6 and 18.6% were dopaminergic and glutamatergic neurons (fig. 5D).

To further explore the function of the dorsal–intermediate lateral septum-to-ventral tegmental area projection, we expressed ChR2-eYFP in the dorsal–intermediate lateral septum GABAergic neurons by injecting an AAV vector carrying ChR2 and eYFP (AAV-Ef1α-DIO-ChR2-eYFP) into the dorsal–intermediate lateral septum of *Vgat-Cre* mice (fig. 5H). In agreement with previous findings, the dorsal–intermediate lateral septum-derived axons were present in the ventral tegmental area (fig. 5I). We performed single-unit recordings in the ventral tegmental area of isoflurane-anesthetized and head-restrained mice (fig. 5H) and activated ChR2-expressing axons near the recording site with 10-ms pulses of light at 20 Hz for 10 s. A total of 115 neurons were recorded. According to waveform principal component analysis and electrophysiologic properties, we eliminated those whose characteristics were unclear; thereafter, the neurons were divided into three groups (Supplemental Digital Content 1, fig. 4, http://links.lww.com/ALN/C642). We found that the firing rate increased in 35%, decreased in 11%, and remained unchanged in 54% of dopaminergic neurons, whereas the firing rate decreased in 55% and remained unchanged in 45% of GABAergic neurons. In addition, the firing rate of 56% glutamatergic neurons did not change, 22% decreased, and 22% increased (fig. 5J). These findings demonstrate that the dorsal–intermediate lateral septum GABAergic neurons send monosynaptic innervations to the ventral tegmental area, preferentially to the GABAergic neurons, which may lead to disinhibition of dopaminergic neurons.

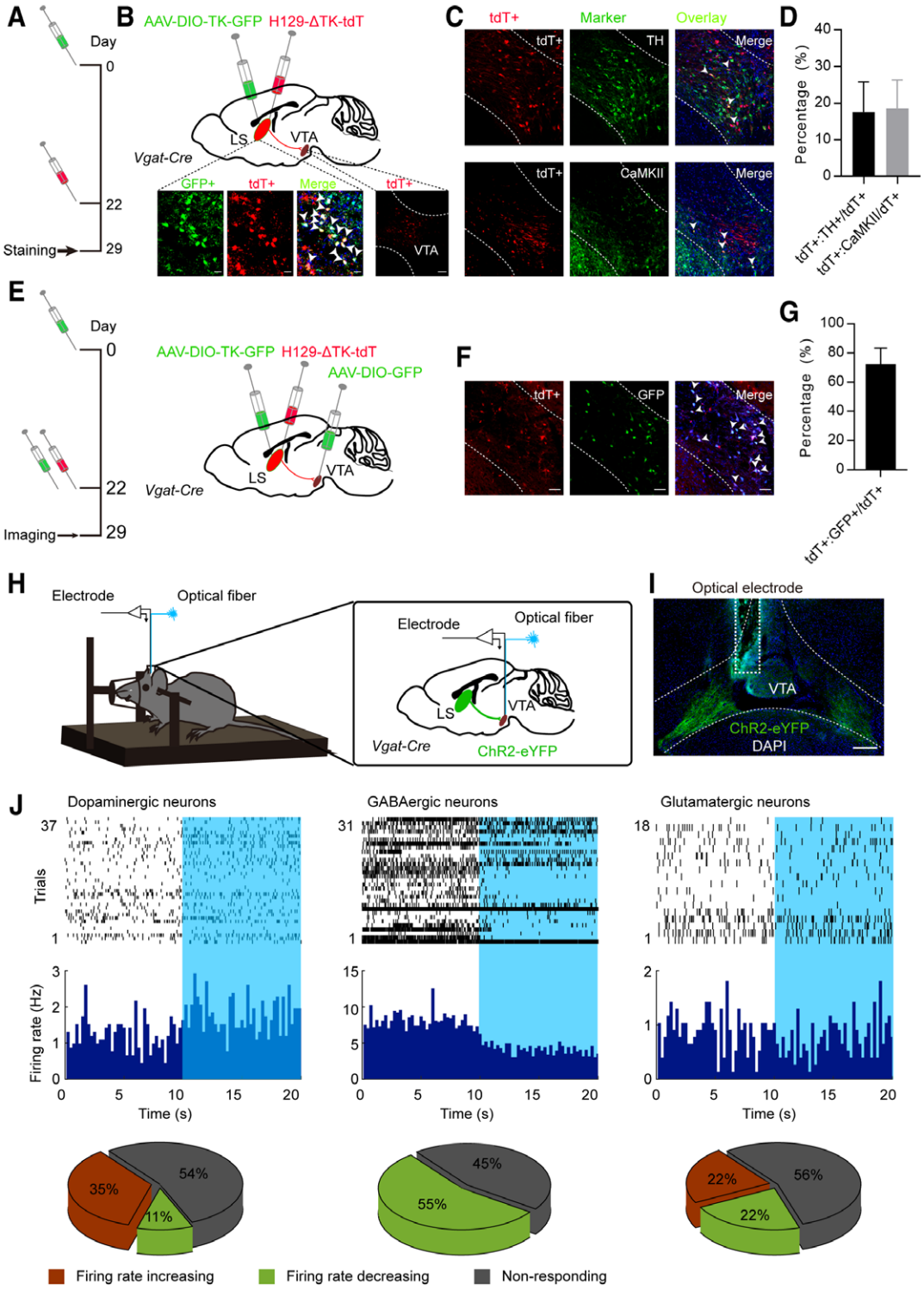

Fig. 5. Dorsal–intermediate lateral septum (LS) γ-aminobutyric acid–mediated (GABAergic) neurons form monosynaptic synapses with ventral tegmental area (VTA) GABAergic neurons. (*A*) Anterograde tracing of the dorsal–intermediate lateral septum-to-ventral tegmental area pathway with the H129-ΔTK-tdT virus. Experimental time line for tracing the lateral septum-to-ventral tegmental area pathway with the helper (adeno-associated virus [AAV]-DIO-TK-GFP, day 0) and H129-ΔTK-tdT (day 22). The brains were obtained on day 29. (*B*) Schematic for virus injection and representative images for the starter neurons indicated by *white arrows* in the dorsal–intermediate lateral septum and tdTomato-positive cells in the ventral tegmental area. The *scale bar* in the lateral septum represents 20 μm. The *scale bar* in the ventral tegmental area represents 100 μm. (*C*) Representative (*Continued*)

Dorsal–Intermediate Lateral Septum GABAergic Neurons Control Wakefulness through the Dorsal–Intermediate Lateral Septum-to-Ventral Tegmental Area Circuit

We wanted to know whether the dorsal–intermediate lateral septum GABAergic neurons contribute to induction of wakefulness through the circuit to the ventral tegmental area. To do this, we expressed GCaMP6s in the dorsal–intermediate lateral septum GABAergic neurons, and the subsequent results indicated that the dorsal–intermediate lateral septum GABAergic neurons send projections to multiple cortical, hypothalamic, and midbrain regions, including the medial prefrontal cortex, hippocampus, anterior hypothalamic area, and periaqueductal gray (not shown). The dorsal–intermediate lateral septum also sends dense axonal collaterals to the ventral tegmental area (Supplemental Digital Content 1, fig. 5B, http://links.lww.com/ALN/C642). The optical fiber was implanted into the ventral tegmental area (Supplemental Digital Content 1, fig. 5, A and B, http://links.lww.com/ALN/C642), and the recordings across vigilance states showed that the axonal calcium signals in the ventral tegmental area were higher in the REM sleep state than in either the awake or non-REM sleep state. Compared with that in the non-REM sleep state, the terminals of dorsal–intermediate lateral septum GABAergic neurons also exhibited higher activities during the awake state (non-REM *vs.* wake: 0.0 [0.0, 0.1] % *vs.* 0.3 [0.3, 0.5] %, $P = 0.035$; non-REM *vs.* REM: 0.0 [0.0, 0.1] % *vs.* 0.8 [0.6, 1.0] %, $P < 0.001$; n = 5 mice/group; Supplemental Digital Content 1, fig. 5, C and D, http://links.lww.com/ALN/C642).

Fig. 5. (*Continued*). immunofluorescence images of the ventral tegmental area slices stained with tyrosine hydroxylase or calcium/calmodulin-dependent protein kinase II. *Scale bar*, 100 μm. (*D*) Statistical results indicating that only 17.6% of tdTomato-positive cells were dopaminergic neurons, whereas 18.6% were glutamatergic neurons. (*E*) Experimental time line. AAV-DIO-TK-GFP and AAV-DIO-GFP were injected into the dorsal–intermediate lateral septum and the ventral tegmental area, respectively, on day 0. H129-ΔTK-tdT was injected into the dorsal–intermediate lateral septum on day 22. The brains were obtained on day 29. (*F*) Representative images of the ventral tegmental area. *Scale bar*, 100 μm. (*G*) Summary showing that 70.7% tdTomato-positive cells in the ventral tegmental area were GABAergic neurons. (*H*) Schematic of the AAV-DIO-channelrhodopsin-2 (ChR2)-enhanced yellow fluorescent protein (eYFP) injection in the dorsal–intermediate lateral septum and the optrode implantation into the ventral tegmental area to simultaneously stimulate the lateral septum axonal terminals in the ventral tegmental area and record the single-unit activities of ventral tegmental area neurons. (*I*) Example image showing the expression of ChR2-eYFP and the location of the optical electrode in the ventral tegmental area. *Scale bar*, 200 μm. (*J*) Example raster and firing-rate histograms of dopaminergic, GABAergic, or glutamatergic neurons after 20-Hz train of light pulses to optogenetically activate the lateral septum GABAergic terminals in the ventral tegmental area. The train begins at 10 s. DAPI, 4′,6-diamidino-2-phenylindole.

In addition, optogenetics was utilized to test the function of the dorsal–intermediate lateral septum-to-ventral tegmental area circuit. ChR2-eYFP or eYFP was expressed in the dorsal–intermediate lateral septum GABAergic neurons of *Vgat-Cre* mice. Two weeks later, fiber optics at a diameter of 200 μm were implanted above the ventral tegmental area. After recovery and habituation, blue light (20 Hz, 2 to 3 mW, 10-ms pulse) was applied for 60 min in the daytime period when the mice were in a sleepy state (fig. 6, A and B). Optical stimulation of the dorsal–intermediate lateral septum-to-ventral tegmental area projections reliably elicited transitions to the awake state from non-REM sleep, as evidenced by the decreased delta power and increased beta power (latency to wake: 139.5 [112.5,168.2] s *vs.* 4.0 [3.3, 4.8] s, $P < 0.001$; delta: 30.1 ± 6.0% *vs.* 16.0 ± 3.4%, $P < 0.001$; theta: 38.5 ± 5.5% *vs.* 35.9 ± 8.6%, $P = 0.553$; Beta: 4.5 [3.9, 5.4] % *vs.* 11.3 [7.3, 11.9] %, $P = 0.050$; gamma: 7.0 [6.0, 9.9] % *vs.* 18.3 [12.4, 23.6] %, $P = 0.109$, n = 6 mice/group; fig. 6, C through H). Meanwhile, terminal stimulation could also accelerate the emergence time from isoflurane anesthesia (468.2 ± 64.1 s *vs.* 149.3 ± 41.7 s, $P < 0.001$, n = 6 mice/group; fig. 6I). In contrast, optogenetic inactivation of the dorsal–intermediate lateral septum GABAergic terminals in the ventral tegmental area promoted the transition from the awake state to non-REM–like sleep state and prolonged the emergence time from isoflurane anesthesia (latency to non-REM: 281.0 [226.7,325.0] s *vs.* 29.0 [24.7, 32.7] s, $P = 0.004$; delta: 25.1 ± 6.6% *vs.* 33.4 ± 3.2%, $P = 0.021$; theta: 42.9 ± 2.5% *vs.* 38.9 ± 2.5%, $P = 0.021$; beta: 5.2 ± 0.9% *vs.* 4.4 ± 0.8%, $P = 0.135$; gamma: 8.2 ± 2.4% *vs.* 5.6 ± 1.6%, $P = 0.054$, n = 6 mice/group; emergence time: 451.0 [416.1, 461.3] s *vs.* 863.5 [745.7, 930.9] s, $P = 0.004$; Supplemental Digital Content 1, fig. 6, A through I, http://links.lww.com/ALN/C642). These results suggest that the dorsal–intermediate lateral septum GABAergic neurons promote wakefulness, at least in part, through their projections to the ventral tegmental area.

Discussion

Our current study demonstrates that the dorsal–intermediate lateral septum GABAergic neurons contribute to the control of wakefulness and anesthesia emergence. Specifically, activation of dorsal–intermediate lateral septum GABAergic neurons induces behavioral arousal and decreases the emergence time from isoflurane anesthesia, whereas inactivation of dorsal–intermediate lateral septum GABAergic neurons promotes non-REM–like sleep state and prolongs emergence time. Anterograde tracing results indicated that the dorsal–intermediate lateral septum GABAergic neurons mainly target GABAergic neurons in the ventral tegmental area. In particular, this projection mediates, at least in part, the effects of the dorsal–intermediate lateral septum GABAergic neurons on behavioral arousal and emergence time from isoflurane anesthesia.

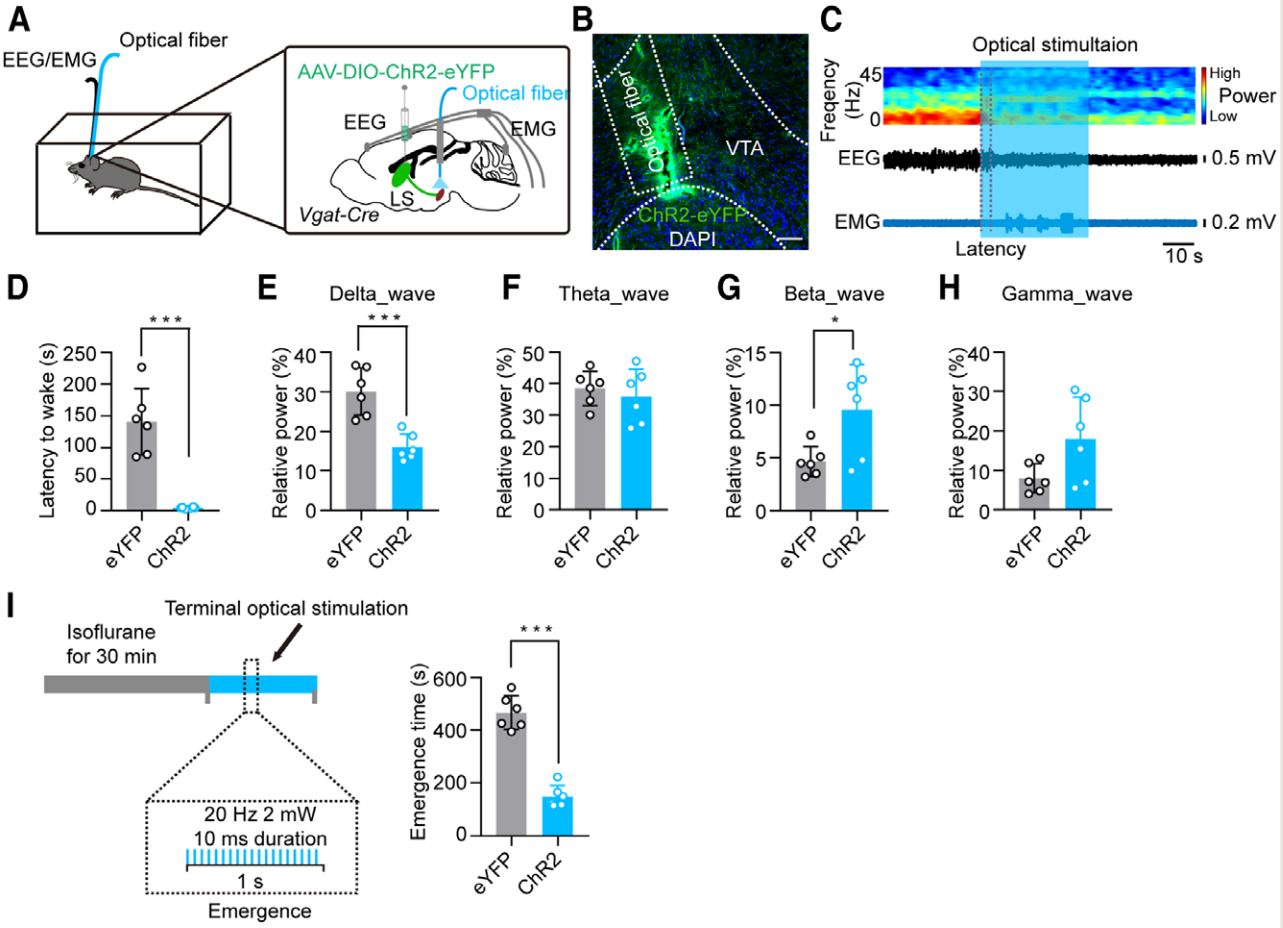

Fig. 6. Optogenetic activation of the dorsal–intermediate lateral septum (LS) γ-aminobutyric acid–mediated (GABAergic) neuronal terminals in the ventral tegmental area (VTA) promoted wakefulness and shortened emergence time from general anesthesia. (*A*) Schemetic showing the virus injection into the dorsal–intermediate lateral septum and optical fiber implantation into the ventral tegmental area. (*B*) Typical image showing the GCaMP6s-labeled neuronal terminals in the ventral tegmental area and the location of the optical fiber. *Scale bar*, 100 μm. (*C*) Representative traces of electroencephalogram (EEG)/electromyography (EMG) recordings and EEG spectrum analysis showing an immediate sleep-to-wakefulness transition during non–rapid eye movement (non-REM) sleep after acute photostimulation (20 Hz for 30 s) of the dorsal–intermediate lateral septum GABAergic terminal in the ventral tegmental area. (*D*) Summary showing that compared to the enhanced yellow fluorescent protein (eYFP) mice (*gray*), the channelrhodopsin-2 (ChR2) mice (*blue*) exhibited lower latencies to wake from non-REM sleep after optogenetic stimulation at 20 Hz. $U = 0.00$, $P < 0.001$, Mann–Whitney rank sum test (two-tailed). (*E* through *H*) Statistical results for power distribution of EEG frequency bands of delta, theta, beta, and gamma during optogenetic activation of dorsal–intermediate lateral septum GABAergic terminals in the ventral tegmental area. Unpaired two-tailed *t* test, delta: $t_{10} = 5.02$, $P < 0.001$; theta: $t_{10} = 0.61$, $P = 0.553$; Mann–Whitney rank sum test (two-tailed), beta: $U = 6.00$, $P = 0.050$; gamma: $U = 8.00$, $P = 0.109$. (*I*) *Left*: Schematic of sustained optical stimulation protocol after the discontinuation of isoflurane administration. *Right*: Summary data showing that activation of the dorsal–intermediate lateral septum GABAergic neuronal terminals in the ventral tegmental area accelerated emergence time from isoflurane anesthesia. $t_{10} = 10.21$, $P < 0.001$, unpaired two-tailed *t* test. The data represent means ± SD. *$P < 0.05$; ***$P < 0.001$. DAPI, 4′,6-diamidino-2-phenylindole.

Mice are nocturnal animals.[32] The lateral septum has close connections with multiple brain regions associated with biologic rhythm cycles, such as the suprachiasmatic nucleus,[33,34] supraoptic nucleus,[28] and paraventricular nucleus.[35] In line with this, we found that c-Fos expression in the lateral septum was higher during nighttime than during daytime. Similarly, many subregions of the midline thalamus are closely associated with the circadian cycle. For example, the levels of c-Fos expression in the paramedian thalamus after periods of sleep, wakefulness, and extended wakefulness are distinctly different.[36] Additionally, it has been suggested that these brain regions are involved in the regulation of mood, pain, cognition, addiction, and other related behaviors.[37,38] This point reminds us that we should

pay attention to the time consistency in these studies to eliminate the bias brought by biologic rhythm cycle.

Understanding the underlying mechanisms for sleep–wake and general anesthesia is one of the most challenging problems in neuroscience. There are several apparent similarities between sleep–wake and anesthesia (anesthesia emergence). For example, EEG recordings of individuals under anesthesia (especially in stage 2 of anesthesia) resemble those associated with non-REM sleep, including 0.5- to 4-Hz delta waves.[21] Our current study demonstrates that the lateral septum GABAergic neurons are mainly wakefulness-promoting neurons, and their activation reduces the depth of anesthesia and promotes recovery from general anesthesia, suggesting a common function of the lateral septum GABAergic neurons in sleep–wakefulness and general anesthesia. However, inhibiting these GABAergic neurons played a much smaller role in promoting sleep-only indirectly promoted non-REM–like sleep state. In fact, it was difficult to further inhibit the lateral septum through a photogenetic technique to deepen the anesthesia when the lateral septum neurons were deeply inhibited by anesthetics. It should be noted that the mechanisms for sleep and anesthesia are not always consistent. Vanini *et al.*[39] recently demonstrated that activation of preoptic GABAergic (sleep-promoting) or glutamatergic (wakefulness-promoting) neurons altered sleep–wake architecture but not anesthetic state transitions, which is different from the traditional classical theory. Although controversies remain, it is beneficial for us to explore how anesthetics induce general anesthesia by unveiling the mystery of sleep. There are sex differences in the regulation of some behaviors, including defensive behavior and maternal behavior, in the lateral septum.[40–42] Few studies have explored sex differences in sleep–wakefulness and general anesthesia mechanism. Nonetheless, it still is a limitation of this study that only male mice were used as research subjects in this experiment.

The roles of dorsal–intermediate lateral septum GABAergic neurons in regulating sleep–wakefulness and anesthesia may depend on their projection patterns: the lateral septum projects to multiple brain regions involved in arousal and motivation, including the ventral tegmental area and hypothalamus, and receives projections from the brainstem and all cornu ammonis areas.[14,15] The ventral tegmental area comprises three types of neurons: dopaminergic, GABAergic, and glutamatergic neurons. Recent studies have shown that dopaminergic and glutamatergic neurons in the ventral tegmental area are essential for the initiation and maintenance of wakefulness,[4,8] and dopaminergic neurons in the ventral tegmental area also participate in behavioral arousal from anesthesia.[43] In addition, ventral tegmental area GABAergic neurons play an important role in the regulation of non-REM sleep. These neurons also facilitate the induction and maintenance and postpone recovery from isoflurane anesthesia.[16,44] Ventral tegmental area dopaminergic and glutamatergic neurons are regulated by GABA from both extrinsic and intrinsic origins.[45] The lateral septum contains mainly GABAergic neurons associated with different neuropeptides,[46,47] and it is a source of GABAergic input to the anterior part of the ventral tegmental area.[30] Maeda and Mogenson[48] showed that the lateral septum stimulation activates a significant number of ventral tegmental area dopaminergic neurons. Recently, Luo *et al.*[14] showed the existence of a functional circuit from the hippocampus through the caudo-dorsal lateral septum to the ventral tegmental area that links context to reward to finally regulate goal-directed behavior. Vega-Quiroga *et al.*[15] also suggested that the lateral septum modulates dopaminergic activities in the antero-ventral region of the ventral tegmental area by inhibiting GABAergic interneurons bearing $GABA_A$ receptors containing the α1 subunit. These findings indicate that the disinhibition of ventral tegmental area GABAergic interneurons through a GABA–GABA connection between the lateral septum and ventral tegmental area is responsible for the increased activities of ventral tegmental area dopaminergic neurons.[49] In line with these results, our data clearly showed predominant anatomic and functional connections between the dorsal–intermediate lateral septum GABAergic neurons and the three types of neurons in the ventral tegmental area. Anterograde tracing further confirmed the innervations from the dorsal–intermediate lateral septum GABAergic neurons onto the ventral tegmental area GABAergic neurons. The finding by optogenetics combined with *in vivo* electrophysiologic methods gave another potent evidence that ventral tegmental area GABAergic neurons were the main targets of the dorsal–intermediate lateral septum GABAergic neurons. It should be noted that the midbrain dopaminergic neurons also project to the lateral septum,[50] which means that the lateral septum and ventral tegmental area are reciprocally connected and thus form a loop that may control sleep and wakefulness. This point warrants further studies in the future. We also mapped the outputs of dorsal–intermediate lateral septum GABAergic neurons in a whole-brain scale. The results reveal that the dorsal–intermediate lateral septum projects to the periaqueductal gray, lateral hypothalamic area, and ventrolateral preoptic nucleus, all of which are involved in sleep–wake states and anesthesia regulation. In this study, we only explained the role of the lateral septum-ventral tegmental area circuit in the regulation of arousal and general anesthesia, and the role of other circuits of lateral septum projection in the regulation of arousal and general anesthesia needs to be further explored. Collectively, our current study unmasks an essential role for the dorsal–intermediate lateral septum GABAergic neurons in promoting wakefulness and anesthesia emergence and points out that the dorsal–intermediate lateral septum-to-ventral tegmental area circuit, at least in part, underlies the effects of the dorsal–intermediate lateral septum GABAergic neurons on physiologic arousal and anesthesia emergence.

Acknowledgments

The authors thank Peng Wu, Ph.D., Cui Yin, Ph.D. and Lingyun Hao, Ph.D. (Jiangsu Province Key Laboratory of Anesthesiology, Jiangsu Province Key Laboratory of Anesthesia and Analgesia Application Technology, Xuzhou Medical University, Xuzhou, China) for expert assistance, and Yan Su, M.D., Feng Dai, M.D., Shi-Ya Zou, M.D., Bing-Qian Fan, M.D., Li Yang, M.D. and Sun-Hui Xia, M.D. (Jiangsu Province Key Laboratory of Anesthesiology, Jiangsu Province Key Laboratory of Anesthesia and Analgesia Application Technology, Xuzhou Medical University) for technical support. The authors also thank Editage (www.editage.com) for English language editing.

Research Support

Supported by National Natural Science Foundation of China (Beijing, China) grant Nos. 81720108013, 31771161, and 81230025 (to Dr. Cao), 81200859 (to Dr. Ding), and 81500950 (to Dr. Yang); "Xing-Wei" Project of Jiangsu Province Department of Health (Jiangsu, China) grant Nos. RC2007094 and XK201136; Jiangsu Provincial Special Program of Medical Science (Jiangsu, China) grant No. BL2014029; Natural Science Foundation of Jiangsu Province (Jiangsu, China) grant No. BK20171159 (to Dr. Ding); Key Project of Nature Science Foundation of Jiangsu Education Department (Jiangsu, China) grant No. 17KJA320005 (to Dr. Ding); Jiangsu Province Ordinary University Graduate Innovation Plan (Jiangsu, China) grant No. KYCX19_2228 (to Dr. Wang); and by funds from Priority Academic Program Development of Jiangsu Higher Education Institutions.

Competing Interests

The authors declare no competing interests.

Correspondence

Address correspondence to Dr. Cao: Affiliated Hospital of Xuzhou Medical University, Xuzhou 221002, China. caojl0310@aliyun.com.

References

1. Trent NL, Menard JL: The ventral hippocampus and the lateral septum work in tandem to regulate rats' open-arm exploration in the elevated plus-maze. Physiol Behav 2010; 101:141–52
2. Albert DJ, Wong RC: Hyperreactivity, muricide, and intraspecific aggression in the rat produced by infusion of local anesthetic into the lateral septum or surrounding areas. J Comp Physiol Psychol 1978; 92:1062–73
3. Lee MG, Hassani OK, Alonso A, Jones BE: Cholinergic basal forebrain neurons burst with theta during waking and paradoxical sleep. J Neurosci 2005; 25:4365–9
4. Eban-Rothschild A, Rothschild G, Giardino WJ, Jones JR, de Lecea L: VTA dopaminergic neurons regulate ethologically relevant sleep–wake behaviors. Nat Neurosci 2016; 19:1356–66
5. España RA, Berridge CW: Organization of noradrenergic efferents to arousal-related basal forebrain structures. J Comp Neurol 2006; 496:668–83
6. Brown RE, Sergeeva OA, Eriksson KS, Haas HL: Convergent excitation of dorsal raphe serotonin neurons by multiple arousal systems (orexin/hypocretin, histamine and noradrenaline). J Neurosci 2002; 22:8850–9
7. Bayer L, Eggermann E, Serafin M, Saint-Mleux B, Machard D, Jones B, Mühlethaler M: Orexins (hypocretins) directly excite tuberomammillary neurons. Eur J Neurosci 2001; 14:1571–5
8. Yu X, Li W, Ma Y, Tossell K, Harris JJ, Harding EC, Ba W, Miracca G, Wang D, Li L, Guo J, Chen M, Li Y, Yustos R, Vyssotski AL, Burdakov D, Yang Q, Dong H, Franks NP, Wisden W: GABA and glutamate neurons in the VTA regulate sleep and wakefulness. Nat Neurosci 2019; 22:106–19
9. Luo YJ, Li YD, Wang L, Yang SR, Yuan XS, Wang J, Cherasse Y, Lazarus M, Chen JF, Qu WM, Huang ZL: Nucleus accumbens controls wakefulness by a subpopulation of neurons expressing dopamine D1 receptors. Nat Commun 2018; 9:1576
10. Naganuma F, Kroeger D, Bandaru SS, Absi G, Madara JC, Vetrivelan R: Lateral hypothalamic neurotensin neurons promote arousal and hyperthermia. PLoS Biol 2019; 17:e3000172
11. Saper CB, Chou TC, Scammell TE: The sleep switch: hypothalamic control of sleep and wakefulness. Trends Neurosci 2001; 24:726–31
12. Uschakov A, Gong H, McGinty D, Szymusiak R: Sleep-active neurons in the preoptic area project to the hypothalamic paraventricular nucleus and perifornical lateral hypothalamus. Eur J Neurosci 2006; 23:3284–96
13. Sherin JE, Shiromani PJ, McCarley RW, Saper CB: Activation of ventrolateral preoptic neurons during sleep. Science 1996; 271:216–9
14. Luo AH, Tahsili-Fahadan P, Wise RA, Lupica CR, Aston-Jones G: Linking context with reward: A functional circuit from hippocampal CA3 to ventral tegmental area. Science 2011; 333:353–7
15. Vega-Quiroga I, Yarur HE, Gysling K: Lateral septum stimulation disinhibits dopaminergic neurons in the antero-ventral region of the ventral tegmental area: Role of GABA-Aα1 receptors. Neuropharmacology 2018; 128:76–85
16. Chowdhury S, Matsubara T, Miyazaki T, Ono D, Fukatsu N, Abe M, Sakimura K, Sudo Y, Yamanaka A:

GABA neurons in the ventral tegmental area regulate non–rapid eye movement sleep in mice. eLife 2019; 8:e44928
17. Ogino Y, Kawamichi H, Saiot S: [Anesthesia and consciousness]. Masui 2016; 65:489–94
18. Allada R: An emerging link between general anesthesia and sleep. Proc Natl Acad Sci USA 2008; 105:2257–8
19. Scammell TE, Arrigoni E, Lipton JO: Neural circuitry of wakefulness and sleep. Neuron 2017; 93:747–65
20. Murillo-Rodriguez E, Arias-Carrion O, Zavala-Garcia A, Sarro-Ramirez A, Huitron-Resendiz S, Arankowsky-Sandoval G: Basic sleep mechanisms: An integrative review. Cent Nerv Syst Agents Med Chem 2012; 12:38–54
21. Brown EN, Lydic R, Schiff ND: General anesthesia, sleep, and coma. N Engl J Med 2010; 363:2638–50
22. Cao JL, Covington HE III, Friedman AK, Wilkinson MB, Walsh JJ, Cooper DC, Nestler EJ, Han MH: Mesolimbic dopamine neurons in the brain reward circuit mediate susceptibility to social defeat and antidepressant action. J Neurosci 2010; 30:16453–8
23. Lee RS, Steffensen SC, Henriksen SJ: Discharge profiles of ventral tegmental area GABA neurons during movement, anesthesia, and the sleep–wake cycle. J Neurosci 2001; 21:1757–66
24. Ungless MA, Magill PJ, Bolam JP: Uniform inhibition of dopamine neurons in the ventral tegmental area by aversive stimuli. Science 2004; 303:2040–2
25. Mohr RA, Chang Y, Bhandiwad AA, Forlano PM, Sisneros JA: Brain activation patterns in response to conspecific and heterospecific social acoustic signals in female plainfin midshipman fish, *Porichthys notatus*. Brain Behav Evol 2018; 91:31–44
26. Aravanis AM, Wang LP, Zhang F, Meltzer LA, Mogri MZ, Schneider MB, Deisseroth K: An optical neural interface: *In vivo* control of rodent motor cortex with integrated fiberoptic and optogenetic technology. J Neural Eng 2007; 4:S143–56
27. Olds J, Milner P: Positive reinforcement produced by electrical stimulation of septal area and other regions of rat brain. J Comp Physiol Psychol 1954; 47:419–27
28. Menon R, Grund T, Zoicas I, Althammer F, Fiedler D, Biermeier V, Bosch OJ, Hiraoka Y, Nishimori K, Eliava M, Grinevich V, Neumann ID: Oxytocin signaling in the lateral septum prevents social fear during lactation. Curr Biol 2018; 28:1066–78.e6
29. Oishi Y, Lazarus M: The control of sleep and wakefulness by mesolimbic dopamine systems. Neurosci Res 2017; 118:66–73
30. Jonsson S, Morud J, Stomberg R, Ericson M, Söderpalm B: Involvement of lateral septum in alcohol's dopamine-elevating effect in the rat. Addict Biol 2017; 22:93–102
31. Zeng WB, Jiang HF, Gang YD, Song YG, Shen ZZ, Yang H, Dong X, Tian YL, Ni RJ, Liu Y, Tang N, Li X, Jiang X, Gao D, Androulakis M, He XB, Xia HM, Ming YZ, Lu Y, Zhou JN, Zhang C, Xia XS, Shu Y, Zeng SQ, Xu F, Zhao F, Luo MH: Anterograde monosynaptic transneuronal tracers derived from herpes simplex virus 1 strain H129. Mol Neurodegener 2017; 12:38
32. Jensen TL, Kiersgaard MK, Sørensen DB, Mikkelsen LF: Fasting of mice: A review. Lab Anim 2013; 47:225–40
33. Ogata R, Ikari K, Matsushima M: Terminal degeneration in the lateral septum of the rat after suprachiasmatic nucleus lesion. Folia Psychiatr Neurol Jpn 1982; 36:163–72
34. Krout KE, Kawano J, Mettenleiter TC, Loewy AD: CNS inputs to the suprachiasmatic nucleus of the rat. Neuroscience 2002; 110:73–92
35. Oldfield BJ, Hou-Yu A, Silverman AJ: A combined electron microscopic HRP and immunocytochemical study of the limbic projections to rat hypothalamic nuclei containing vasopressin and oxytocin neurons. J Comp Neurol 1985; 231:221–31
36. Ren S, Wang Y, Yue F, Cheng X, Dang R, Qiao Q, Sun X, Li X, Jiang Q, Yao J, Qin H, Wang G, Liao X, Gao D, Xia J, Zhang J, Hu B, Yan J, Wang Y, Xu M, Han Y, Tang X, Chen X, He C, Hu Z: The paraventricular thalamus is a critical thalamic area for wakefulness. Science 2018; 362:429–34
37. Williams NR, Taylor JJ, Lamb K, Hanlon CA, Short EB, George MS: Role of functional imaging in the development and refinement of invasive neuromodulation for psychiatric disorders. World J Radiol 2014; 6:756–78
38. Goedecke L, Bengoetxea X, Blaesse P, Pape HC, Jüngling K: μ-Opioid receptor-mediated downregulation of midline thalamic pathways to basal and central amygdala. Sci Rep 2019; 9:17837
39. Vanini G, Bassana M, Mast M, Mondino A, Cerda I, Phyle M, Chen V, Colmenero AV, Hambrecht-Wiedbusch VS, Mashour GA: Activation of preoptic GABAergic or glutamatergic neurons modulates sleep–wake architecture, but not anesthetic state transitions. Curr Biol 2020; 30:779–87.e4
40. Wong LC, Wang L, D'Amour JA, Yumita T, Chen G, Yamaguchi T, Chang BC, Bernstein H, You X, Feng JE, Froemke RC, Lin D: Effective modulation of male aggression through lateral septum to medial hypothalamus projection. Curr Biol 2016; 26:593–604
41. Lee G, Gammie SC: $GABA_A$ receptor signaling in the lateral septum regulates maternal aggression in mice. Behav Neurosci 2009; 123:1169–77
42. Helmy M, Zhang J, Wang H: Neurobiology and neural circuits of aggression. Adv Exp Med Biol 2020; 1284:9–22
43. Taylor NE, Van Dort CJ, Kenny JD, Pei J, Guidera JA, Vlasov KY, Lee JT, Boyden ES, Brown EN, Solt K: Optogenetic activation of dopamine neurons in

the ventral tegmental area induces reanimation from general anesthesia. Proc Natl Acad Sci USA 2016; 113:12826–31

44. Yin L, Li L, Deng J, Wang D, Guo Y, Zhang X, Li H, Zhao S, Zhong H, Dong H: Optogenetic/chemogenetic activation of GABAergic neurons in the ventral tegmental area facilitates general anesthesia via projections to the lateral hypothalamus in mice. Front Neural Circuits 2019; 13:73
45. Tan KR, Rudolph U, Lüscher C: Hooked on benzodiazepines: $GABA_A$ receptor subtypes and addiction. Trends Neurosci 2011; 34:188–97
46. Risold PY, Swanson LW: Chemoarchitecture of the rat lateral septal nucleus. Brain Res Brain Res Rev 1997; 24:91–113
47. Sheehan TP, Chambers RA, Russell DS: Regulation of affect by the lateral septum: Implications for neuropsychiatry. Brain Res Brain Res Rev 2004; 46:71–117
48. Maeda H, Mogenson GJ: Electrophysiological responses of neurons of the ventral tegmental area to electrical stimulation of amygdala and lateral septum. Neuroscience 1981; 6:367–76
49. Nieh EH, Vander Weele CM, Matthews GA, Presbrey KN, Wichmann R, Leppla CA, Izadmehr EM, Tye KM: Inhibitory input from the lateral hypothalamus to the ventral tegmental area disinhibits dopamine neurons and promotes behavioral activation. Neuron 2016; 90:1286–98
50. Khan S, Stott SR, Chabrat A, Truckenbrodt AM, Spencer-Dene B, Nave KA, Guillemot F, Levesque M, Ang SL: Survival of a novel subset of midbrain dopaminergic neurons projecting to the lateral septum is dependent on NeuroD proteins. J Neurosci 2017; 37:2305–16